ADVANCED FUNCTIONAL MATERIALS
www.afm-journal.de

Resilin in Insect Flight Systems

Esther Appel, Jan Michels, and Stanislav N. Gorb**

Compared to wingless insects, pterygote insects profit from numerous wing-related benefits including a wider distribution range, the exploitation of various food resources and the escape from water- or land-confined predators. In order to maintain the wings´functionality, the wing design and resistance to material fatigue are of key importance. This is even more essential for survival when considering that wings are used for millions of wing beat cycles but cannot be repaired and do not contain inner muscles so that their aerodynamic performance is mainly based on passive, structure-based wing deformations. One of the components serving this purpose is the endowment of certain wing components with the elastomeric protein resilin building stable and complex material composites with the tanned cuticle. Resilin endows the respective structures with, e.g., higher flexibility and compliance and enables elastic energy storage. In this study, the occurrence of resilin in the insect flight system is reviewed based on previous studies of several insect orders including Odonata, Orthoptera, Hymenoptera, Coleoptera, Dermaptera, and Diptera, and the function of resilin is discussed with reference to the respective structures.

1. Introduction

Elastomeric proteins occur in a wide range of organisms, ranging from elastin in vertebrates, gluten in plants, abductin in bivalve molluscs to resilin in arthropods.[1] They endow the respective system with elasticity and longevity and show a broad spectrum of mechanical properties, depending on, e.g., their degree of structural (dis-)order and their linkage to other molecules via specific binding domains.[2] Whereas spider silk is known for its unmatched toughness and elastin for its exceptional durability, resilin exhibits an almost perfect resilience of 92–97% and, therefore, has often been called "rubber-like protein."[1,3]

Resilin is a disordered protein and mainly occurs in the insect exoskeleton, where it is linked to chitin via a Rebers and Riddiford chitin-binding domain. It has a low stiffness (Young's modulus of 0.6–2.0 MPa), can be extended to more than three times of its original length and has a high fatigue limit of over 300 million cycles as well as the ability of elastic energy storage and damping.[2–8] Apart from its high resilience and durability, low stiffness, and high extensibility, it also features high heat- and solvent-stability, high biocompability and biodegradability, a lack of immunogenicity, multi-stimuli responsiveness and the ability to self-assemble.[2–9,10] Due to this combination of various advantageous properties, the development of resilin-like polypeptides (RLPs) and modular RLPs for various medical and industrial applications in bioadhesive and tissue engineering, drug delivery, biosensor techniques, bioimaging, catalysis, and hydrogel bioelectronics has been strongly advanced since the report of the synthesis of the first recombinant pro-resilin in 2005.[7,9] The potential to readily change the RLPs' responsiveness to various stimuli (like pH, temperature [RLPs exhibit a dual-phase transition behavior], mechanical stress, ions, etc.) and to influence its capability to self-assemble by changing the amino acid composition, the hydropathy index and the number and length of elastic repeat motifs are only one of many advantages of resilin-like polypeptides.[9,10] As the original RLPs lack properties such as cellular adhesion and proliferation, the development of tunable modular RLPs with additional secondary domains further widened the range of potential fields of applications.[9,10] Since the synthesis of the first modular RLP in 2009 (RLP_{12}-RGD_2-MMP-HBD) that was equipped with a fibronectin cell-binding sequence (RGD), a matrix metalloproteinase-sensitive sequence (MMP) for proteolytic degradation and a heparin-binding domain (HBD) for heparin or growth factor immobilization and controlled release, various different modular RLPs with functional, bioactive domains as well as structural domains have been synthesized.[9,10,11] For example, modular RLPs with an integrin-binding sequence (RGD) for cell adhesion and insertions of lysine residues as crosslinking sites were used in combination with a thiol-cleavable crosslinker.[12] The latter can be cleaved in the presence of reducing agents that commonly occur in, e.g., tumors, thereby creating a soft, biocompatible, selectively degradable hydrogel that can be used for drug delivery and as tissue engineering scaffold.[12] The combination of RLP blocks and hydrophobic elastin-like polypeptide (ELP) blocks was shown to

E. Appel, J. Michels, S. N. Gorb
Functional Morphology and Biomechanics
Zoological Institute
Kiel University
Am Botanischen Garten 1-9, D-24118 Kiel, Germany
E-mail: eappel@zoologie.uni-kiel.de; sgorb@zoologie.uni-kiel.de

The ORCID identification number(s) for the author(s) of this article can be found under https://doi.org/10.1002/adfm.202215162

DOI: 10.1002/adfm.202215162

create stable spherical micelles that can be used for drug delivery as well.[9,13] By varying the RLP block repeat number and the ELP block hydrophobicity, it was shown that a minimum number of RLP blocks is necessary for self-assembly into micelles, that an increasing RLP number can further modulate their size and that increasing the ELP-hydrophobicity promotes the formation of cylindrical instead of spherical micelles.[13] Other studies showed that combining the cellulose-binding module (CBM) and the amphiphilic hydrophobin protein domain (HFBI) with an RLP region in between not only allows for the design of nanocomposite biomaterials with, e.g., nanocrystalline cellulose and for an increase in coacervate size, but also enables the testing of the RLP's mechanical response to a change in, e.g., pH by attaching the modular RLP to a cellulose substrate (via CBM) and an AFM cantilever (via HFBI).[9,14,15] Additionally, RLPs can be used to form nanobioconjugates with platinum noble metal quantum clusters, acting as structure-directing and reducing, stabilizing agent for the synthesis of precise nanoclusters.[16] Furthermore, modular RLPs can also be used for the purification of proteins by adding multiple RLP repeats to a target protein, e.g., the enhanced green fluorescence protein (EGFP), and taking advantage of the RLP's upper critical solution temperature (at around 6 °C) while conducting a cold-temperature coacervation.[17] Therefore, designing modular RLPs not only endows biomaterials with desired bioactivity, mechanical properties and modified stimuli-responsiveness as well as enhanced crosslinking, self-assembly and self-healing, but also facilitates purification and selective biodegradation.

During the last decades, various putative resilin-like proteins have been identified, but not all of them might exhibit the surpassing rubber-like elasticity known from the resilin samples tested so far. Apart from the microscopical and mechanical analyses described below, the amino acid sequence of proresilins provides useful information about, e.g., the translocation (the uncrosslinked pro-resilin is secreted into the extracellular space), potential binding partners, the structure and the potential elasticity of a protein.[19] With the identification of the *Drosophila Dm-CG15920* gene and the production of a synthetic resilin with long-range elasticity by using it as template, several important regions of a standard pro-resilin have been identified and can be used as reference for the comparison with putative resilin-like pro-resilins.[7,19–22] Beginning from the N-terminal region, the *Drosophila* pro-resilin features 1) a signal peptide (MFKLLGLTLL MAMVVLG or variants), which allows the transport of the protein to the extracellular space, 2) a glycine- and proline-rich, elasticity-endowing region—the exon I peptide—, containing 18 relatively short A-repeats, which consist of the sequence GGRPSDSYGA PGGGN or variations of it, 3) an extended Rebers & Riddiford consensus sequence of type RR-2 (*YDNDE*PAKYE FNYQVEDAPS GLSFGHSEMR DGDFTTGQYN VLLPDGRKQI VEYEADQQGY RPQIRYEG*DA NGGSGPSGP* (The exact range of the R&R sequence is still not clear. Inconsistent amino acids are italicized.), which enables the protein to bind to chitin (The RR-2 type does normally occur in proteins of sclerotized, hard cuticles, and the RR-1 type is typically present in soft cuticles, but so far the RR-2 type has been found in most of the analyzed pro-resilins.), though there is also a slicing variant without chitin-binding domain, 4) a glycine- and proline-rich, elasticity-endowing region—the exon III peptide—containing ten B-repeats, consisting of the sequence GYSGGRPGGQDLG or variations of it, and 5) a relatively high content of tyrosine allowing for the formation of dityrosine and trityrosine crosslinks (**Figure 1**A,B).[7,19–24] These crosslinks link the randomly coiled polymer chains to a network structure and hinder the stretched polymer chains from irreversibly sliding past each other and, therefore, have a major contribution in resilin's surpassing resilience.[19,25–27] The covalent bonds are very stable, even when exposed to acid hydrolysis.[27] In standard pro-resilin, tyrosine is distributed regularly throughout the repeat sequences, and 20–25% of the tyrosine is used for crosslinking with around 40–60 residues separating the crosslinks.[2,7,28] Trityrosine crosslinks are assumed to increase the protein's stiffness, and the ratio of dityrosine-to-trityrosine crosslinking was supposed to depend on, e.g., the deposition time (before/after ecdysis, at day/night) and temperature conditions (constant/changing).[27–30]

When putative resilin-like proteins lack the signal peptide, have only very few or no repeats (A higher amount of repeats increases the potential extent of extensibility/stretching.), show a high content of alanine together with a low content of glycine or proline, exhibit a reduced amount of tyrosine or completely lack a chitin-binding-domain, they should be critically reviewed.[19] For example, an increased proportion of alanine (e.g., above 20%) favors the formation of turns (helix-stabilizing effect), thereby increases the protein's stiffness and often occurs in proteins of hard, sclerotized cuticle.[19]

Analyses of the two repeat-containing regions revealed that the exon I peptide is probably located outside the cell membrane and has a resilience of around 90% (93% when cross-linked; termed "soft segment"), whereas the exon III peptide is suggested to be located inside the cell membrane and to have a resilience of around 63% (86% when cross-linked; termed "hard segment").[23,24] Qin and co-workers suggested that upon stress application, the super-elastic soft segment is readily deformed and transfers energy to the hard segment, which transforms to more ordered beta-structural conformations.[24] In contrast to structurally ordered proteins like collagen or keratin, whose elastic recoil relies on the change in internal energy upon deformation of the protein's structure, the main driving force in structurally disordered proteins like resilin, elastin, silk or abductin is a change in entropy, favoring the protein's relaxed state with the maximum amount of potential polymer chain configurations (Figure 1C).[2]

Key factors for the rubber-like behavior of resilin are a high chain length combined with a high degree of chain flexibility and mobility based on the presence of structure-disrupting amino acids for ensuring a large deformability and spatial flexibility in the relaxed state and to promote entropy-driven elastic recoil from the stressed state.[2] Resilin's pronounced chain flexibility is based on the high repetitiveness of certain low-complexity amino acid sequences with a high amount of glycine (30–40%) and proline (7–13.5%).[1,19,31] Whereas glycine, with its single hydrogen side chain, bestows the polymer chains with high conformational flexibility, the heterocyclic ring of proline is connected to the protein backbone twice, thereby leading to a high conformational rigidity. Therefore, if present in large amounts, both amino acids act as structural disrupters, resulting in a near-absence of any extended secondary structure like hydrogen-bonded β-sheets or α-helices.[1,2,20,25,31,32] Instead, resilin's characteristic

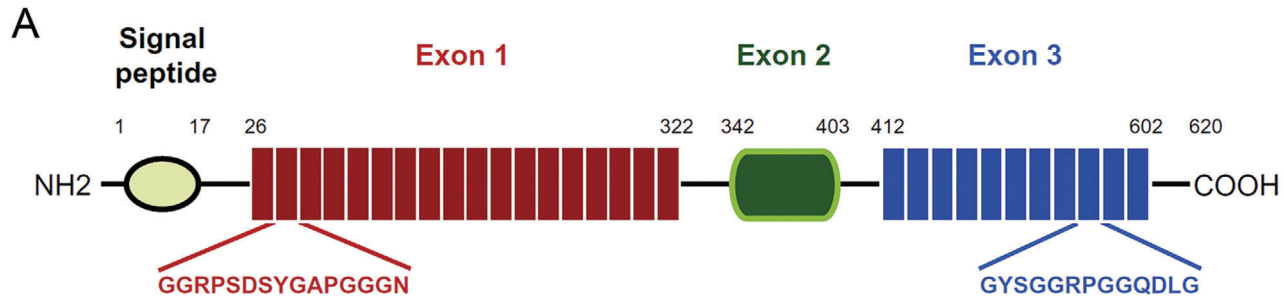

B

MFKLLGLTLL	MAMVVLGRPE	PPVNSYLPPS	DSYGAPGQSG	PGGRPSDSYG	APGGGNGGRP	SDSYGAPGQG 70
QGQGQGQGGY	AGKPSDTYGA	PGGGNGNGGR	PSSSYGAPGG	GNGGRPSDTY	GAPGGGNGGR	PSDTYGAPGG 140
GGNGNGGRPS	SSYGAPGQGQ	GNGNGGRSSS	SYGAPGGGNG	GRPSDTYGAP	GGGNGGRPSD	TYGAPGGGNN 210
GGRPSSSYGA	PGGGNGGRPS	DTYGAPGGGN	GNGSGGRPSS	SYGAPGQGQG	GFGGRPSDSY	GAPGQNQKPS 280
DSYGAPGSGN	GNGGRPSSSY	GAPGSGPGGR	PSDSYGPPAS	GSGAGGAGGS	GPGGADYDND	EPAKYEFNYQ 350
VEDAPSGLSF	GHSEMRDGDF	TTGQYNVLLP	DGRKQIVEYE	ADQQGYRPQI	RYEGDANDGS	GPSGPGGPGG 420
QNLGADGYSS	GRPGNGNGNG	NGGYSGGRPG	GQDLGPSGYS	GGRPGGQDLG	AGGYSNGKPG	GQDLGPGGYS 490
GGRPGGQDLG	RDGYSGGRPG	GQDLGASGYS	NGRPGGNGNG	GSDGGRVIIG	GRVIGGQDGG	DQGYSGGRPG 560
GQDLGRDGYS	SGRPGGRPGG	NGQDSQDGQG	YSSGRPGQGG	RNGFGPGGQN	GDNDGSGYRY	620

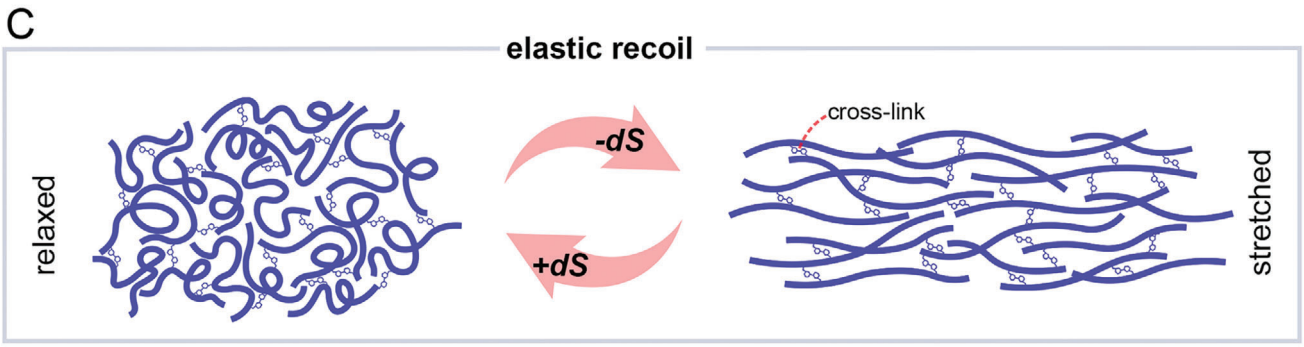

Figure 1. Amino acid sequence and elasticity mechanism of resilin. A) *D. melanogaster* CG15920 pro-resilin protein sequence with signal peptide (in yellow), N-terminal elastic domain (in red), Rebers & Riddiford 2 consensus sequence (in green) and C-terminal elastic domain (in blue). Reproduced with permission.[22] Copyright 2014. B) Amino acid sequence of *D. melanogaster* CG15920 pro-resilin (obtained by UniProt) with signal peptide (in yellow), A-repeats-containing region (in red) (after,[22] 2014), R&R2 sequence (in green) (after,[19] 2010, and the cuticleDB website http://bioinformatics2.biol.uoa.gr/cuticleDB/) and B-repeat-containing region (in blue) (after[22]). Repeat sequences are underlined (after,[19] 2010). C) Scheme of the mechanism of resilin's elasticity relying on a change in entropy and favoring the relaxed state with maximum potential chain configurations.

amino acid sequence leads to a high propensity for more flexible conformations like the highly hydrated polyproline II helices in the stretched state and β-turns in compression, resulting in a decrease in overall polymer stiffness and an increase in backbone hydration by water, thereby decreasing protein aggregation and promoting elastic recoil.[2,4,33–36] The effect of an increasing amount of glycine and proline in changing the main driving force for elastic recoil from internal energy to entropy by increasing the structural disorder was shown for spider silk by comparing the ampullate and flagelliform silks of different araneid spiders, i.e., the spidroin-1 fibroins containing ampullate silk of *Nephila clavipes* with a reduced proline content of 3.5% and the spidroin-2 fibroins containing flagelliform silk of *Araneus diadematus* with a higher amount of proline residues of 16%.[37,38] The authors showed that an increase in the amount of proline from 3.5% to 16% in glycine-rich silks (45% glycine in spidroin-1 fibroins and 40% in spidroin-2 fibroins) is enough to change the elastic recoil from 100% internal-energy-driven (by at least 10% extension, *N. clavipes*) to 100% entropy-driven (*A. diadematus*).[38] By comparing the proline and glycine composition of various elastomeric protein domains and amyloids, Rauscher and co-workers revealed that there is a linear threshold of proline and glycine content above which the majority of these sequences belongs to structurally disordered, entropically recoiled proteins and that around two glycines have the same effect as one proline in elastin.[34] The amount of glycine and

proline in the standard resilin samples of different insect species in most cases varies within a range of 30–40% for glycine and 7–13.5% for proline.[19] Nevertheless, there are also proteins like the XP_002428637.1 *Pediculus humanus* protein, which contain much less glycine (12.1%) but can still be classified as resilin-like protein due to, e.g., the existence of a signal peptide, which enables the transport to the extracellular matrix, a R&R consensus sequence of type RR-2 and an A-repeat-containing region containing six nearly identical repeats.[19] The lower amount of glycine and repeats, however, might indicate that the peptide chains are not as mobile and flexible as in standard glycine-rich (pro-)resilins.[19] Additionally, a higher amount of alanine (as present in several examined putative resilin-like proteins, e.g., XP_002428637.1 with an amount of 10.4% versus CG15920-PA with an amount of 4.8%) in repeat regions might lead to the formation of a series of turns and finally to the protein being stiffer and less rubber-like.[19]

Together with glycine and proline, hydrophobic amino acid residues like alanine, valine, leucine, isoleucine, and phenylalanine make up a proportion of around 66% in standard resilins, which is lower than in other elastomeric proteins like silk or elastin.[10] In comparison to collagen and elastin, resilin contains an increased amount of hydrophilic amino acid residues like glutamic acid, aspartic acid, arginine, and lysine with more acidic than basic side chains. This leads to a decrease in protein-protein interactions and an increase in hydration, amounting to 50–60% at a pH value of 7, as well as to a low isoelectric point at around a pH value of 4–5, where swelling is minimum.[4,19,33,39,40]

In summary, the local manifestation of resilin's mechanical properties highly depends on 1) environmental factors, such as hydration level (and, therefore, the supply with hemolymph) and motion frequency, whether it is mainly used in tension or compression, 2) the amount and directional arrangement of embedded chitin fibers, 3) the structure of the polypeptide chains, including, e.g., the amount of single amino acids like glycine and proline, 4) the abundance of resilin with and without a chitin-binding domain, and 5) the density and ratio of dityrosine to trityrosine cross-linking.[18,19,21,27,41–45] Recently, Lerch and coworkers compared the distribution of Pro-Resilin-GFP and dityrosine bonds in fruit flies and showed that in some areas signal intensities did not match, supporting the assumption that there is a varying activity of cross-linking enzymes controlling the dityrolisation and thereby changing the extent of resilin's elasticity in different tissues.[46] Furthermore, they suggested the term "Resiliome" to refer to a composite resilin matrix composed of not only resilin, but other presumably elastic cuticular proteins with Rebers & Riddiford chitin-binding domain (Cpr) like the *Drosophila* Cpr56F protein, as well, thereby modulating the degree of elasticity.[46] This assumption is i.a. based on the fact that some dityrosine signals were still present in resilin-less flies, that Cpr56F-GFP and Pro-Resilin-GFP signals partly matched, that pro-resilin, in contrast to Cpr56F, is not expressed in the elastic cuticle of larval stages and that a reduced or eliminated pro-resilin expression leads to nonlethal mutants (in contrast to elastin mutants in mice), suggesting that other elastic proteins compensate for resilin´s elasticity in pro-resilin mutants.[46] However, further studies are needed so that we further refer to resilin as it is the most thoroughly studied protein of the resilin matrix.

Apart from differences regarding the properties of resilin (matrices) itself, very often, resilin-bearing structures exhibit a gradient in the material composition with a transition from areas of virtually pure resilin to chitin-dominated areas with an increasing proportion of chitin and an increasing degree of sclerotization, and this is reflected in the presence of a stiffness gradient.[1,3,47] In many structures, like in the adhesive tarsal setae of beetles, such a stiffness gradient—from 1.2 MPa at the tip to 6.8 GPa near the base of the seta—can considerably improve the system's performance.[47] However, when analyzing biological resilin samples for their stiffness, the proportions of resilin and chitin as well as the arrangement of the chitin fibers have to be considered in the interpretation of the results. For example, a dragonfly tendon consisting of virtually pure resilin has an elastic modulus of 0.6–0.7 MPa, whereas a locust prealar arm with around 24% of chitin and 76% of resilin was shown to have an elastic modulus of around 0.9–2.0 MPa and to deform three times less in longitudinal stretching than in compression or bending due to the arrangement of chitin lamellae.[3–6,48]

In order to analyze the presence and distribution of resilin, a variety of methods can be used. In contrast to most of the other exoskeleton parts, resilin is colorless, transparent, and amorphous and, thereby, can sometimes be discerned even with the naked eye.[4] It exhibits an anisotropic swelling when immersed in water (especially due to its high content of proline, glycine, and hydrophilic groups) and becomes birefringent when being tensioned in a hydrated condition.[2,4] When dried or dehydrated, resilin becomes solid, glass-like and brittle but can be rehydrated within seconds to minutes.[4,33] As resilin's covalent crosslinks of di- and trityrosine show a relatively pronounced violet/blue autofluorescence when excited with UV light (with excitation and emission maxima of 320 nm and 415 nm, respectively), it can also be visualized with fluorescence microscopy, given that appropriate filter sets are available.[49–51] As described by Michels and Gorb, confocal laser scanning microscopy can be used to not only analyze the distribution of resilin but also to get an overview about the general material composition of a cuticular structure.[51] They used four different excitation wavelengths ranging from 405 to 639 nm (together with respective filters) to excite and detect four autofluorescences, to which they allocated different colors. Overlays created from data obtained by this method show the following color code and are also used in this work: blue colors indicate resilin-dominated areas, green colors indicate the dominance of non- or only weakly-sclerotized chitinous material, and red colors indicate structures dominated by strongly sclerotized chitinous material.[51–53] Additionally, different dyes have been shown to stain resilin, e.g., Masson and Mallory dyes (resilin is stained red) or methylene blue and toluidine blue dyes (resilin is stained violet/blue).[3,51,54,55]

Since its first description by Weis-Fogh in 1960, resilin has been found in various arthropod systems, including joint and neck membranes, elastic springs, tendons, leg and wing vein joints, inner layers of wing veins as well as in tarsal attachment pads and setae, mouthparts, reproductive organs, and mechanoreceptors.[4,51,56–60] In these structures, resilin serves, e.g., the storage of elastic energy, the reduction of stress concentration and material fatigue, the generation of flexibility and adaptability and the improvement of damping properties.[4,52–54,56,57,61–66]

In the insect flight system, resilin-containing structures are subjected to a variety of forces at different frequencies and occur in various forms from bulky chunks to delicate fold or flexion lines and in nearly pure state or as composites with neatly layered chitin fibers to fulfill a large range of specialized functions. In order to maintain the functionality and efficiency of their wings even after millions and millions of cycles, insects have evolved an elaborate wing structure with a refined network of veins and a relief to influence the wing's directional rigidity and to increase the aerodynamic efficiency, a circulatory system for nutrient and water supply, a sensory apparatus for accurately monitoring external and internal signals and a composite material of varying stiffness, ranging from a few MPa to several GPa, depending on, e.g., the amounts of resilin and chitin and the extent of sclerotization. Before we discuss the occurrence and function of resilin in different structures of the insect flight system, the following section focuses on the aforementioned adaptations of the insect wing in order to allow analyzing resilin-supported structures in terms of a wider structural and biological context.

Insect flight evolved about 400 million years ago.[67,68] The insect wings' evolutionary origin and development are not fully resolved yet.[69] Several studies have examined the wing development during organogenesis and morphogenesis, including the imaginal ecdysis and expansion, up to the removal of apoptotically dissolved epidermal cells and the connection of the two cuticular wing halves.[70–80] In contrast to the still widespread assumption that mature wings are mostly non-living tissue, wings are far from being plain dead appendages. After the connection of the two wing halves, their hollow veins stay connected to the circulatory body system. They contain hemolymph, tracheae, and nerves, which enable the wing's supply with oxygen, water, hormones, nutrients, and other important substances as well as the removal of metabolic products.[79,81,82] Hemolymph is transported out of the wing with the help of accessory pulsatile organs creating a global bulk flow pattern, which can be circuitous or tidal.[79–81,83,84] The local flow behavior in wings is quite complex, involving cross and longitudinal veins as well as some membranous areas, and can be characterized as pulsatile, continuous, or leaky, with each flow pattern predominating in different areas of the wing.[79–81,85] Recently, tracheation, which until then had been assumed to be restricted to the wing veins, was even found within the wing membrane of a dragonfly.[86]

The importance of the circulatory system within wings becomes clear when considering the drastic changes in mechanical properties of a hydrated versus a desiccated wing. The latter rapidly loses weight and flexibility, its stiffness and toughness increase, and it becomes brittle.[87–93] This has also been reported for wings of aged insects, in which circulation slows down and some veins even lack hemolymph.[81,94,95,96] Apart from, e.g., the reduced flexibility in joints or other resilin-containing structures, it can be one of the reasons for wing fracture in the predominantly affected posterior part and trailing edge of dragonfly wings.[79,97–99] Furthermore, recent studies by Hou and coworkers[100,101] suggest that due to the hemolymph and its differently distributed mass throughout the wing, the moment of inertia should be considered to increase by around 50% and the center of mass should be shifting anteriorly and is probably different from what has been shown by Norberg,[102] thereby influencing wing pitch, the onset of flutter and, therefore, the critical flight speed.

Additionally, hemolymph circulation, as well as tracheal and neural connections, are also important for the complex multimodal sensory apparatus of insect wings.[79] Receptors are mainly located at veins or joints and often contain resilin (e.g., at the basis of flexible mechanoreceptors). Wings show a variety of receptor types, including 1) mechanoreceptors like a) hair sensilla at the margins of the wings, which detect air-borne vibrations, b) campaniform sensilla at various locations on the wing, which measure wing cuticle deformations, c) stretch and chordotonal proprioreceptors at the wing base, which monitor wing movements and influence wing beat rhythmicity (stretch receptors) and encode vibrations during flight (chordotonal receptors), d) auditory organs (tympanal organs) at the wing base used in the intraspecific communication and predator detection, 2) chemoreceptors (gustatory receptors) at the leading edge and 3) thermoreceptors, which prevent overheating by influencing wing folding.[79] Recently, Fabian and co-workers[103] mapped the route of axons with terminal soma as well as the distribution of eight classes of sensory structures (including, e.g., single- and double-innervated hair sensilla, campaniform sensilla, hair plate sensilla and chordotonal organs) on the dorsal and ventral sides of dragonfly and damselfly wings in particular detail. Their study showed the existence of over 750 sensors on each dragonfly wing (and around half of this amount in damselfly wings), with the number of sensilla positively scaling with the wing length.[103] They further revealed specific sensilla distribution patterns associated, e.g., with the wing's corrugation, the strain distribution during flight and the position along the wing length and chord, with the wing tip and the posterior wing chord being less densely covered by sensilla.[103]

Maintaining the functionality and efficiency of the wings is of great importance for the survival of pterygote insects as it assures the access to food sources, enables the animals to escape more easily from predators and opens up a wider distribution and migration range. Additionally, wings do not only serve locomotion but are also used for sound production,[104–107] thermoregulation,[108,109] visual communication,[110–112] orientation[79] or, in a more sclerotized, derived form, as a protective covering for the tightly folded and packed hindwings of some insect orders.[113,114] To fulfill all these functions and maintain the wings' functionality, wing structure and resistance to failure are of key importance, especially when considering that insect wings 1) do not contain inner muscles so that their aerodynamic performance is mainly based on passive deformations with only some support of the muscles attached to the wing base and 2) are made only once during lifetime and cannot be repaired.[98,115,116] Considering that the life span of an adult flying insect ranges from several hours or days up to years and that insects flap their wings with wing beat frequencies of 20 to over 1000 Hz (*Schistocerca gregaria* vs *Forcipomya* sp.), often several hours a day and, therefore, millions and millions of cycles, the latter is even more astonishing.

During the past few decades, many studies have elucidated how wings of different insect orders are adapted to these tasks.[52,53,97–99,116–119] Although insect wings are diverse in size, shape, number, density and arrangement of longitudinal and cross veins as well as resilin-containing flexion and fold lines and

flexible joints (which lead to varying wing bending and torsion during flight) and are used at different wing beat frequencies and with different muscular control, all of them have certain characteristics in common, which especially improve their mechanical stability, flexibility, and flight efficiency.

Insect wings normally show a high relief at their anterio-proximal part, which serves as rigid support to resist higher bending moments.[116,120] Towards the wing tip (and often towards the trailing edge), the relief diminishes in the form of decreasing wing corrugation, membrane thickness, vein diameter, or the complete absence of veins, thereby increasing the flexibility of the wing tip (in which inertial forces peak at stroke reversal), in order to 1) reduce stresses at the wing base, 2) minimize energy expenditure for wing acceleration and 3) reduce damages from impact forces.[116,120,121]

Another wing characteristic is the existence of large-scale camber, small-scale corrugation or both.[116,118,122,123] Camber formation can be influenced by certain wing structures, such as the arculus in dipteran and odonatan wings, flexion lines in, e.g., hymenopteran or megalopteran wings (like the median flexion line, which can also be partly controlled basally by muscles attached to the axillae), or simply by wing torsion or spanwise transversal corrugation, which makes the wing more flexible in chordwise than in spanwise direction.[116,122,123] Such a 3D shape has an effect on the flexural and torsional rigidity of the wing, mostly creating a ventrally concave and a dorsally convex wing side at downstroke (and a slightly reversed camber during the upstroke).[116,122,123] This asymmetry increases the resistance to the aerodynamic forces (with a maximum at mid-stroke) and the manifold higher inertial forces (with a maximum at stroke reversal) applied from the concave wing side in comparison to the convex wing side.[116,120,121] When the aerodynamic and inertial forces are centered behind the torsional axis (thought, the maximum of aerodynamic forces lies closer to the anterior wing part), the camber also induces asymmetric wing twisting, with the wing twisting more during supination than during pronation.[102,116,124–126]

Camber formation has been shown to improve the aerodynamic efficiency (lift-to-drag-ratio) of a wing in several studies, although Engels and co-workers[127] stated that its influence on the temporal distribution of aerodynamic forces particularly relies on the change of the effective angle of attack.[127–131] If small-scale corrugation, apart from improving the wing's stiffness against bending and influencing its deformation, also increases its aerodynamic efficiency, is still under debate.[127,128,130,132–143] There are indications that corrugation valleys can trap vortices and stagnant air cushions and thereby contribute to improve lift production,[134,138] but smaller scale corrugation, spanwise flow advecting vorticity, low Reynolds numbers and high angles of attack decrease the probability of trapping vortices in flapping wings.[127,140,142,143]

In all these above-mentioned structures and processes, resilin plays a more or less important role in ensuring, e.g., directional deformation and adaptability, elastic energy storage, the reduction of stress concentration, and the increase of fracture resistance. In the following sections, we will summarize the results on the existence and function of resilin in various structures of the insect flight apparatus of different insect orders. Starting with the three structures described in the pioneer study of Weis-Fogh in 1960, a dragonfly tendon, a locust wing hinge ligament and a locust prealar arm, we will further continue with the insect orders Odonata, Hymenoptera, Coleoptera, Dermaptera, and Diptera.

1.1. Elastic Dragonfly Tendon

One of the first resilin-bearing structures described by Weis-Fogh in 1960 is a sausage-like swelling of the thoracic tendon for the pleuro-subalar muscle in the dragonfly flight apparatus.[4] In *Aeshna grandis* (Linnaeus, 1758), the swollen part of the tendon, called elastic tendon, has a length of about 0.7 mm and a width of about 0.15 mm and was assumed to consist of 99% resilin.[4] In the native state, it is surrounded by thick hypodermal cells and their basement membrane.[4] These cells were assumed to form the tendon in the course of 3 d before the final molt.[3,29] After removing the surrounding tissue, the elastic tendon has a hyaline, colorless appearance and was shown to contain virtually pure resilin (**Figure 2**A). Weis-Fogh described the tendon as a cylindrical tube-like structure consisting of a central epicuticular tube, a thick-walled tube of pure protein and a cortical chitinous tube.[4] While the central and cortical tubes withstand protease digestion, the prominent inner proteinaceous tube was shown to be fully digested.[4] Figure 2B illustrates a virtual 1 µm thick cross section of the dorsal half of the elastic tendon of *Aeshna cyanea* (Müller, 1764) visualized with confocal laser scanning microscopy. Based on differences in the autofluorescence composition of the material, it indicates that the tendon has a threefold layering, with the outer and innermost layers being dominated by autofluorescence shown in green and the bulk material being dominated by autofluorescence shown in blue.

The entire tendon belongs to the group of cap tendons. It is a hollow invagination from the dorsal body wall and ventrally forms a wide cap-like insertion for the pleuro-subalar muscle, which originates from the lower part of the pleuron.[4] Both ends of the tendon are usually rather tough and inextensible, showing a dominant lamellate cuticle structure mainly composed of chitin.[3] At the transition zone between the tough endings and the elastic, resilin-dominated part, resilin first appears in form of irregular patches, interspersed with concentrically arranged chitin lamellae.[3] Further toward the elastic part of the tendon, the chitin-resilin composite takes up the whole cross section, getting more and more devoid of chitin lamellae.[3] On the dorsal end, the tendon is attached to the subalar sclerite via a flexible membrane, which has a complex pattern of microfolds, and is further indirectly connected to the axillary sclerites of the wing base via the subalar sclerite (Figure 2B–D).[4] At the dorsal end of the elastic tendon and in the transition zone towards the flexible membrane, the inner resilin-dominated area of the tendon becomes more and more interspersed with chitin lamellae, and the thin epicuticle begins to show wrinkles, which turn into microfolds at the level of the flexible membrane (Figure 2B).[4]

The elastic tendon can be stretched up to 2.5–3.0 times the swollen length in extension and compressed up to one third without showing any permanent deformation.[4] Being released from the applied force, it shows an instantaneous elastic recovery with resilience (i.e., recovery of the stored elastic energy after deformation) of up to 92% (the resilin-like polypeptide Rec1-Resilin shows a resilience of up to 97%).[4,6–8] It has a fatigue limit of

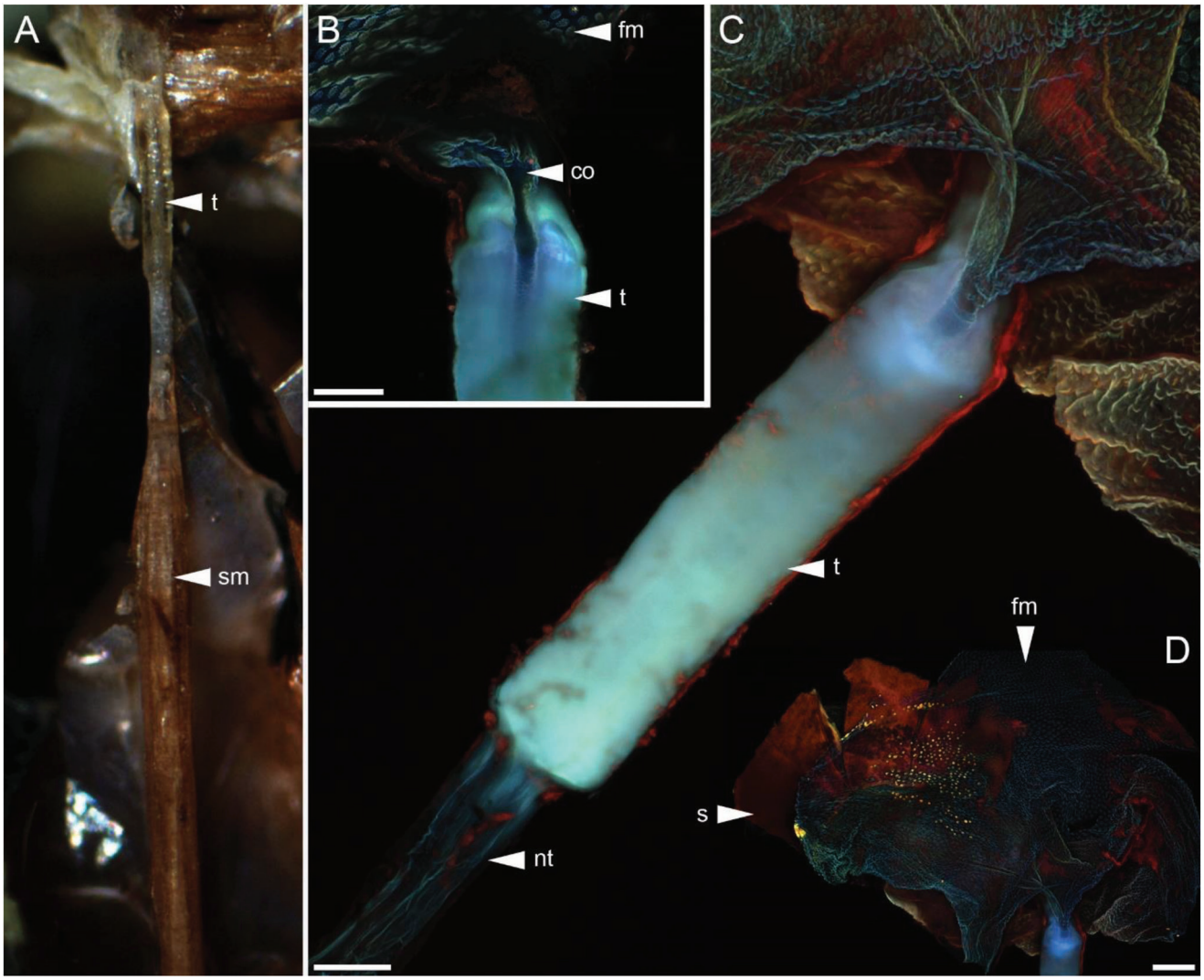

Figure 2. Resilin-bearing thoracic tendon (t) of the pleuro-subalar muscle (sm) in the dragonfly *Aeshna cyanea*. A) Light microscopy. B–D) Confocal laser scanning microscopy (CLSM). B) 1-µm-thick cross section of the tendon showing the tendon´s hollow channel opening (co) toward the dorsal end. The tendon consists of a prominent layer being arranged as a thick-walled tube and featuring dominant autofluorescence shown in blue and a second thinner layer that surrounds the first layer and is dominated by autofluorescence shown in green. Small wrinkles on the inside of the hollow tube turn to more complex microfolds in the dorsally connected membrane. C,D) Maximum intensity projection. C) Tendon in unstretched state with a flexible membrane (fm) on the dorsal side and a non-swollen part (nt) of the tendon on the ventral side. D) Upper part of the tendon connected to sclerites (s) through a flexible membrane (fm) with microfolds. co—channel opening, fm—flexible membrane with microfolds, nt—non-swollen part of the tendon, s— sclerite, sm—subalar muscle, t—elastic tendon. Scale bars: B,C) 50 µm, D) 100 µm.

over 300 million cycles, a tensile strength (stress at the rupture point) of about 3–4 MPa and a stiffness (elastic modulus) of about 0.6–0.7 MPa in extension and compression.[4,144]

During flight, the elastic tendon was assumed to support the role of the anterior coxoalar muscle in controlling wing twisting (i.e., supination) during the upstroke.[3,145,146] While the coxoalar muscle causes supination on the last 10° of the downstroke and during the first part of the upstroke, the pleuro-subalar muscle with the attached tendon controls supination at a later phase of the upstroke.[145] For this, the muscle contracts slowly and tonically and keeps the tendon at a certain length and tension, while the elastic tendon probably takes up wing movements and oscillates in length, showing a large reversible extensibility (e.g., over 250% in the forewing of *Libellula luctuosa* (Burmeister, 1839)) and endowing the structure with a long fatigue life.[145] This mechanism can be particularly beneficial for hovering flight and other flight maneuvers but can also apply during turbulent flows when the wing is subjected to excessive movements.[146]

Recently, Bäumler and Büsse examined the pterothorax of five different dragonfly and damselfly species for the existence of resilin in the cap tendons of their pterothoracic muscles.[147] They showed that resilin can be found in all 20 (21 for Anisoptera) cap tendons of the pterothorax in all investigated species. These cap-tendon-bearing muscles are mostly associated with flight (with the exception of two muscles involved in moving the abdomen) and include phasic muscles, which directly move the wing, as

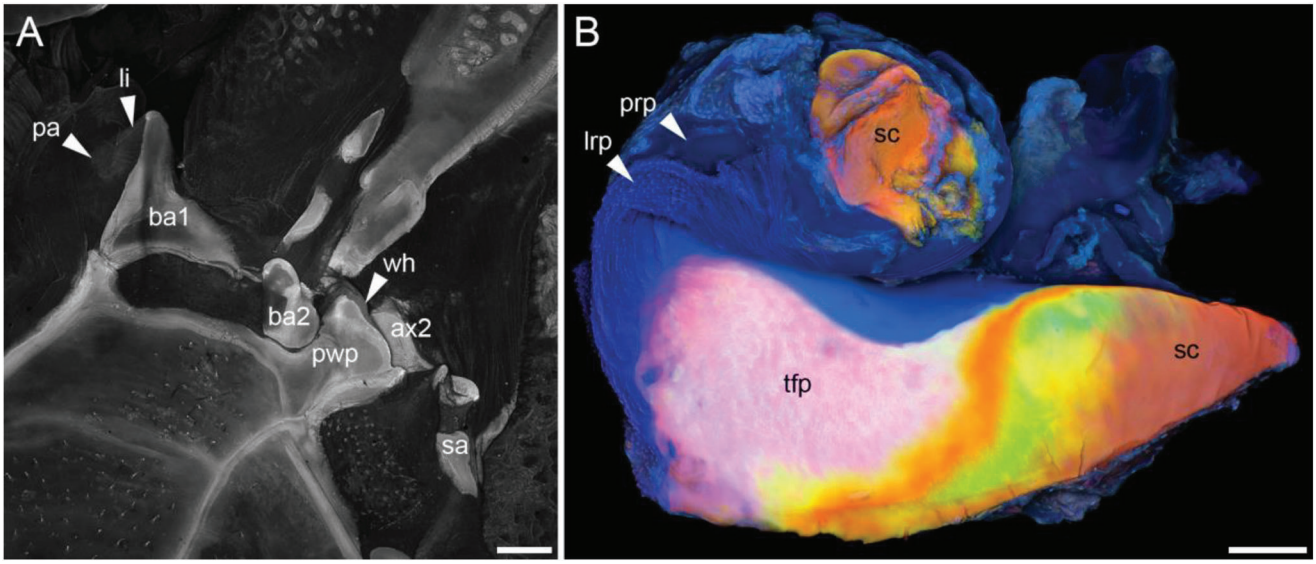

Figure 3. Locust wing hinge ligament. A,B) Confocal laser scanning microscopy. A) Shown in grey scales. A) Wing base with the wing hinge ligament (wh) being connected to the (meso-) pleural wing process (pwp). B) Wing hinge of a female of the locust species *Locusta migratoria*, Reproduced with permission.[51] Copyright 2012, Wiley. Dorsal side consisting of a lamellar rubber-like part (lrp) and a pure resilin part (prp) and ventral side consisting of a tough flexible part (tfp); sclerotized cuticle (sc) is present at the dorsal and ventral ends of wing hinge ligament. ax2—second axillary wing sclerite, ba1—first basalar sclerite, ba2—second basalar sclerite, li—ligament, lrp—lamellar rubber-like part, pa—prealar arm, prp—pure resilin part, pwp—(meso-) pleural wing process, sa—subalar sclerite, sc—sclerotized cuticle, tfp—tough flexible part, wh—wing hinge ligament. Scale bars: A) 500 µm, B) 100 µm.

well as tonic muscles like the pleuro-subalar muscles described above.[147] Except for Odonata, resilin has also been found in tendons of other insects, e.g., in the tergopleural tendon in flies.[148]

1.2. Locust Wing Hinge Ligament

The locust forewing wing hinge ligament is attached to the (meso-) pleural wing process and to another sclerotized process located underneath the second axillary wing sclerite (**Figure 3**A).[3,4] It consists of three different zones: 1) a rather tough, dense and mainly chitinous ventral part, which contains a small amount of resilin (tfp), 2) a soft dorsal part, which is divided into a pad of pure resilin (prp), and 3) a pad of resilin interspersed with chitin lamellae (lrp). The dorsal and ventral ends of the wing hinge ligament are lined by dark, sclerotized cuticle (sc) (Figure 3B).[3,4,51] On its external exposed side, the wing hinge ligament is framed by hypodermal cells.[3,4] The deposition of resilin and chitin lamellae (zone 3) by these hypodermal cells starts at around three days before emergence in the pharate adult.[29,48] After around one week, chitin deposition ends, and only pure resilin (zone 2) is deposited until around three weeks after the final molt.[48] As in the prealar arm (see below), growth layers fluorescing under UV-light can be found in the locust wing hinge ligament, with thin, faintly fluorescent layers formed during the day and wide, brightly fluorescing layers formed each night.[29] Finally, the wing hinge ligament consists of 86% resilin and 14% chitin and residual proteins and was found to have an elastic modulus of around 2.6 MPa.[45,48]

Several studies suggest that the wing hinge ligament is able to absorb tensile and compressive forces.[1,3,54,149] For example, during the upstroke, when the proximal end of the second axillary sclerite rotates around the (meso-) pleural wing process, the wing hinge ligament is stretched and can store kinetic energy at maximum wing deflection.[3,4,150] During the subsequent downstroke, the elastic recoil of the wing hinge ligament can then support wing acceleration.

In contrast to locusts, Lepidoptera, Coleoptera, and some Hymenoptera have tough and inextensible wing hinge ligaments.[3] In these insects, elastic energy storage for wing acceleration can probably be provided by the flight muscles and the rigid thorax cuticle.[1,3] Consistently, several studies suggested that resilin´s resilience might be too small at high wing beat frequencies to serve elastic energy storage, as resilin was mainly found to occur in insects with synchronous flight muscles, a low wing beat frequency of <50 Hz and high inertial forces during the wing beat cycle.[1,3,5,6] However, some small, seemingly resilin-bearing wing hinge ligaments have also been found in *Calliphora*, *Bombus*, *Apis* and *Oryctes* between different sclerites, raising the question whether the high resilience of resilin can also be given at higher wing beat frequencies.[3,151] Since the study by Jensen and Weis-Fogh in 1962, only a few studies have investigated the dynamic mechanical properties of native resilin, and there is still some controversy going on.[3,5,6,45,146,152] While Jensen and Weis-Fogh[5] investigated the prealar arm's frequency-dependent behavior up to a frequency of 200 Hz, King[146] and Choudhury[152] used the technique of time temperature superposition principle (TTSP) with varying frequency, temperature, and hydration level to obtain data for a larger range of frequencies, including a phase transition frequency. In contrast to most other studies that examined resilin in tension, Kovalev and co-workers characterized the mechanical properties of the locust wing hinge ligament in

compression using microindentation and analyzed the data using the poroelasticity theory, a generalized Maxwell model with two characteristic time constants and a 1D model.[45] So far, the data suggest that the cockroach tibia-tarsal joint resilin is less resilient than locust prealar arm resilin and the dragonfly tendon resilin at low frequencies.[5,6,146,152] This might be due to the amount and purity of resilin in the examined structures, with the tendon showing the highest purity. Furthermore, the authors reported that the resilience of resilin test pieces was optimal at low frequencies but seemingly show only some decrease in resilience (≈5–15% of the values measured for around 10 Hz) with increasing frequency of up to 200 Hz (prealar arm resilin not tested at higher frequencies), but a significant decrease from around 600 Hz on (exact values strongly depending on the examined structure; examined: cockroach tibia-tarsal joint resilin, prealar arm resilin and dragonfly tendon resilin).[5,6,146,152] Gosline and co-workers, who measured a frequency range of up to 200 Hz, even inferred that the prealar arm resilin in insect flight systems can only work efficiently as elastic energy storage material at wing beat frequencies at around or below 25 Hz (range of wing beat frequency of, e.g., locusts and dragonflies), at which the resilience is at around 70%.[6] For insects with asynchronous flight muscles and a wing beat frequency in the range of 100 to 700 Hz, they concluded that resilin is probably not playing a major role in elastic-energy storage.[6] Kovalev and co-workers conducted several indents (each with a load application time of 10 to 80 s) within a few minutes and detected that at the second indentation with lower indentation depth, the time-force curve showed an increase instead a decrease in force, a phenomenon that is called inverse stress relaxation and that is linked to viscosity.[45] They concluded that the locust wing hinge ligament might be adapted to both rather fast (e.g., flight, ≈25 Hz, range of milliseconds) and slow (e.g., wing folding, range of seconds) mechanical processes, with relatively fast processes eliciting an elastic response and slow processes showing a viscoelastic behavior.[45] Further examinations are needed to get comparable results with different samples of native resilin at a wide range of frequencies in tension and compression.

1.3. Locust Prealar Arm

The locust prealar arm can be described as a hyaline peg, which is located at the front edge of the mesotergum anterior to the wing base (Figures 3A and 4A–C).[3] It has a diameter of about 250–450 µm and a length of about 500–600 µm, and it is of irregular shape having curved ventral and lateral sides and a V-shaped groove along its dorsal side (**Figure 4**A–D).[3,5] The tip of the prealar arm is connected to the anterior tip of the first basalar sclerite of the pleuron through a thick, tough and flexible ligament (Figures 3A and 4C).[3] Through the connection to the basalar sclerite, the prealar arm is further indirectly connected to the humeral angle of the anterior part of the wing base. The prealar arm features a dark sclerotized base, which shows a relative abrupt transition to the hyaline, resilin-dominated peg, the latter consisting of around 24% chitin and 76% resilin (Figure 4A–D).[3,48] It is composed of thin (<0.2 µm (0.06 µm[153])) concentric chitin lamellae, which are separated by thick (1–3 µm) layers of resilin, resembling the lamellate transition zone in dragonfly tendons.[3,153]

Resilin and chitin are deposited by the surrounding hypodermal cells, which remain constant in number throughout the deposition and secrete chitin or resilin synchronously so that coherent sheets arranged parallel to the hypodermal cell layer can be formed.[5,48] The prealar arm of an 11-day old locust has about 130 chitin lamellae.[48] In contrast to the wing hinge, in which chitin deposition is already ceased one week after emergence with only pure resilin being deposited afterward, in the prealar arm, deposition of both chitin and resilin by the hypodermal cells continues until the formation of the prealar arm is completed (about three weeks).[48] The chitin lamellae seemingly continue into the sclerotized base, thereby probably forming a firm anchoring for the elastic peg.[3]

Due to the arrangement of the chitin lamellae, the prealar arm's deformation in longitudinal direction (extension) is mainly determined by its chitin component and was shown to be about three times less pronounced than in compression at varying stresses.[3,5] During bending and compression, the prealar arm behaves like a pure rubber with its mechanical behavior being predominantly based on the properties of the resilin component.[3,4] Weis-Fogh[4] and Jensen and Weis-Fogh[5] showed that the prealar arm has a static elastic modulus of about 1.96 MPa measured perpendicularly to the chitin fibrils and an elastic modulus of about 0.9–2 MPa.[4–6]

Contraction of the basalar muscle, which is connected to the basalar sclerite, causes wing pronation and depression through the connection to the humeral angle. During muscle contraction, the prealar arm is deformed and stores elastic energy that likely contributes to wing supination.

1.4. Dragonfly Wing Vein Joints and Veins

Wings of dragonflies and damselflies show a corrugated network of slender, short cross veins, which are connected to thick, longwise running longitudinal veins by wing vein joints. These vein joints can be either flexible or fused (**Figure 5**A,B). Flexible vein joints only form a limited contact to the adjacent longitudinal vein and were found to be dominated by resilin.[61,154–156] In contrast, fused vein joints establish a much broader contact to the adjacent longitudinal vein and are dominated by chitinous, sclerotized cuticle.[61,154–156] Flexible vein joints can be secondarily stiffened by so-called spines (or spikes), which are mostly cone-shaped, hollow protrusions (Figure 5C).[61,157,158] Spines are located in direct proximity to and are often directed towards the adjacent longitudinal vein and were supposed to limit the free movement of cross veins around the longitudinal vein, therefore, secondarily providing the vein joint with a directional stiffness.[61,154–156] Nevertheless, spines vary in their proximity to the adjacent longitudinal vein and show a great diversity in shape and size among dragonflies and damselflies and can, therefore, be assumed to have a more or less pronounced effect on limiting the directional rotation around the longitudinal vein.[155]

Finite-element modeling suggested that in contrast to fused joints, which show a high local stress concentration at the connection between cross vein and longitudinal vein, in flexible resilin-bearing joints (i.e., double flexible joints with resilin

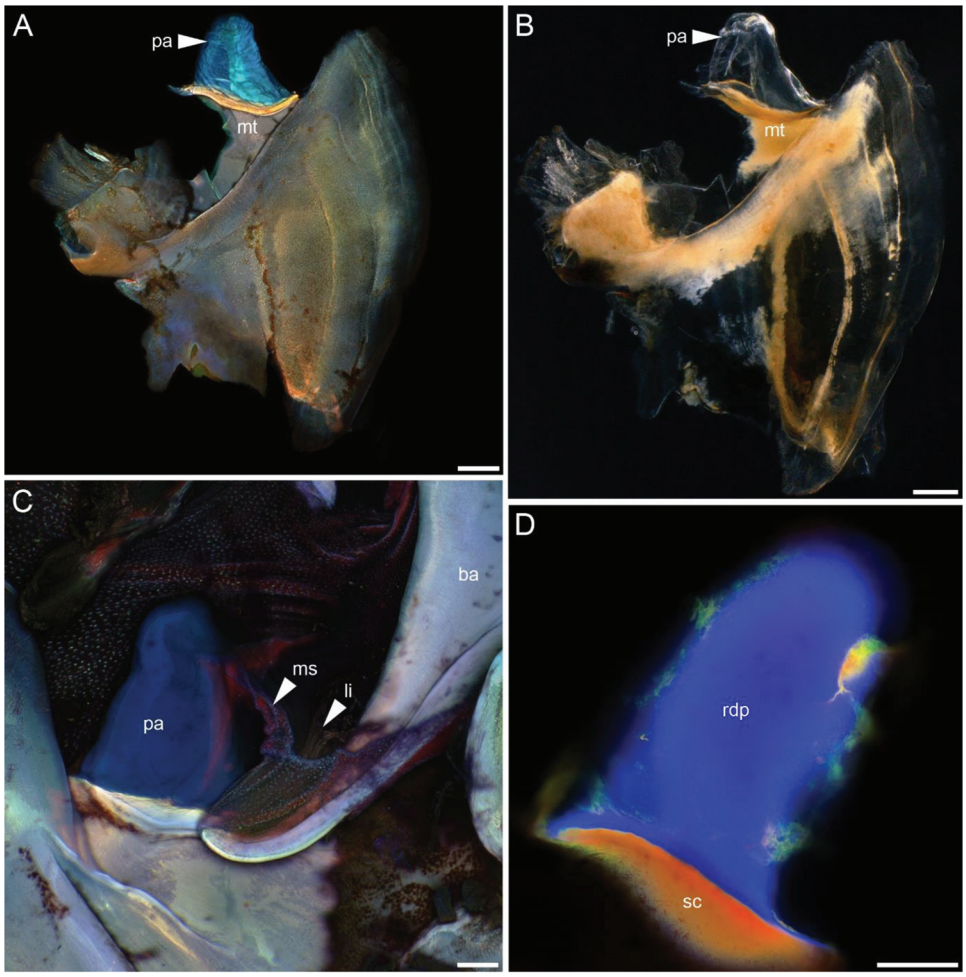

Figure 4. Locust prealar arm. A,C,D) Confocal laser scanning microscopy. B) Light microscopy. A,B) Prealar arm (pa) situated at the front edge of the mesotergum (mt). C) Prealar arm (pa) located on the mesotergum (mt) and connected to the first basalar sclerite (ba) by a ligament (li) and a flexible membranous suspension (ms). D) 6.6 µm thick optical section of the prealar arm with highly sclerotized base (sc) and resilin-dominated part (rdp). Reproduced with permission.[51] Copyright 2012, Wiley. ba—first basalar sclerite, li—ligament, ms—membranous suspension of the prealar arm and first basalar sclerite, mt—mesotergum, rdp—resilin dominated part, sc—sclerotized cuticle. Scale bars: A,B) 200 µm, C,D) 100 µm.

patches on both the ventral and dorsal sides) the stress levels are higher on the adjacent wing membrane and lower on the joint itself, therefore, most probably contributing to the reduction of fatigue-related damages.[160,161] Therefore, resilin can be assumed to reduce stress concentrations at vein joints, thereby preventing failure at higher deformations.[160] As can be seen in Figure 5B, wing membrane cells show a gradient in material composition, with the border area adjacent to the wing veins being dominated by autofluorescence shown in blue and the central area showing an increased proportion of autofluorescence shown in green, suggesting a softer cuticle in the border area.[65] Such a kind of flexible suspension might help reduce stress levels in the connection area between veins and membrane and contribute to delay the tear-off of the wing veins from the membrane.[65]

In a wider context, flexible resilin-bearing vein joints were further assumed to generally contribute to the increased chordwise flexibility of odonatan wings and to play a role in controlling directional passive wing deformations, like promoting the aerodynamically advantageous camber formation during the downstroke.[61,155,156] As insect wings lack internal muscles for precisely controlling the wing form, they largely rely on such passive mechanisms. Donoughe and co-workers[156] and Rajabi and co-workers[160] showed that different joint combinations (consisting of two vein joints, one on the dorsal and another one on ventral side) have a different rotational stiffness, with the double-flexible joint combinations being the most flexible vein joint type.[156,160] Distribution analyses of the different vein joint types and spines on the dorsal and ventral wing sides in different families of Odonata revealed pronounced differences between the Anisoptera and the Zygoptera (but also within the suborders), leading to a classification into five different groups.[155,156,162] Further analyses by Rajabi and co-workers, who analyzed wing sections comprising five vein joints (joint combinations) by finite-element modeling, showed a high degree of variation in the deformation and stress distribution in different wing sections depending on vein joint distribution and occurrence of spines.[163] Furthermore, they demonstrated that the angular deformation

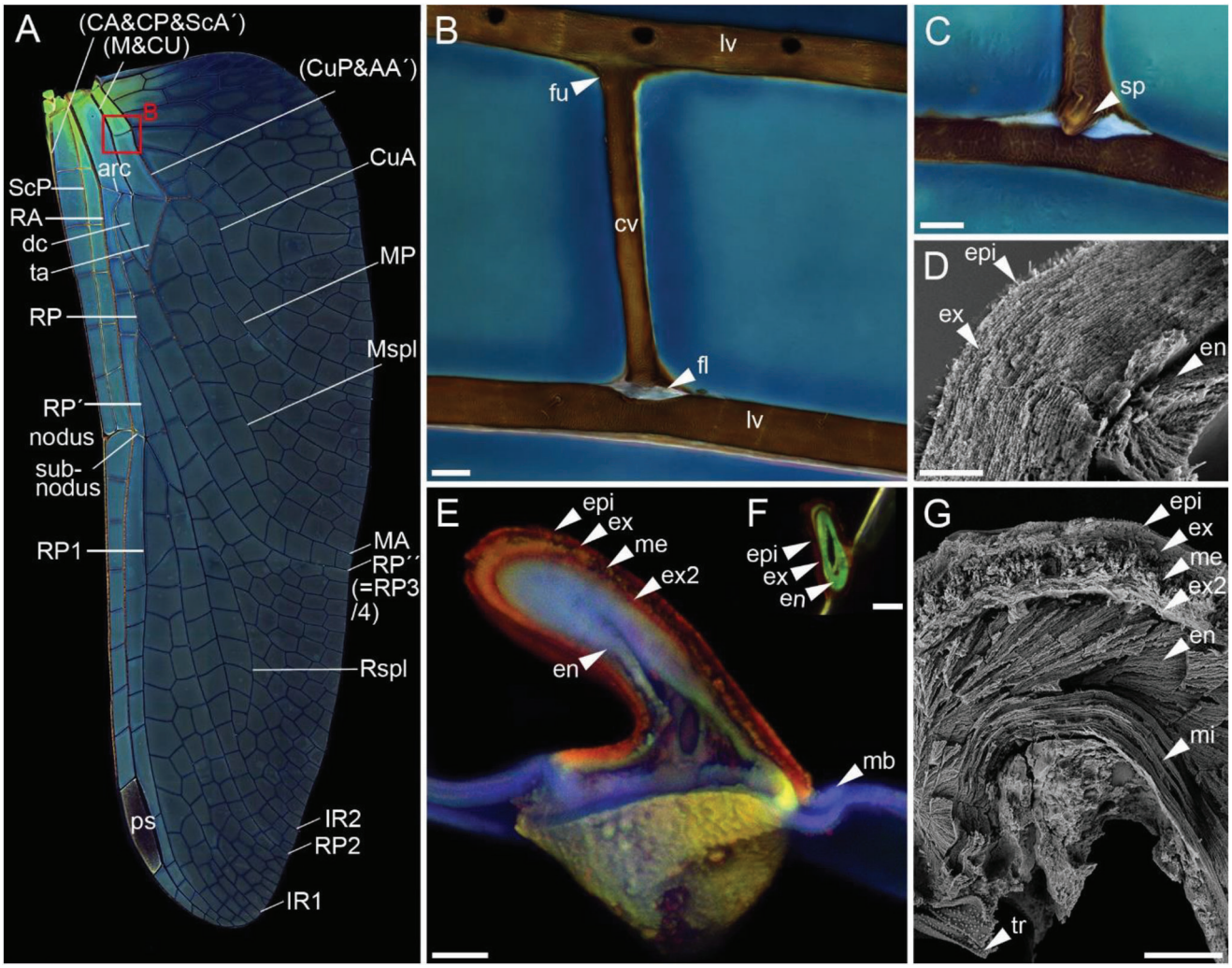

Figure 5. Occurrence of resilin in dragonfly wings. A,B,C,E,F) Confocal laser scanning microscopy. D,G) Scanning electron microscopy. A) Left hind-wing of *Sympetrum vulgatum*, dorsal side; nomenclature of the wing structures after.[159] D–G) Reproduced with permission.[65] Copyright 2015, Wiley. B) Detail of A) (red square) showing a cross vein (cv) being flexibly connected (fl—flexible joint) to an adjacent longitudinal vein (lv) on one end and being fused (fu—fused joint) with a longitudinal vein on the other end. C) Flexible joint with spine (sp) directed towards the longitudinal vein. D) Cross section of a cross vein consisting of epicuticle (epi), exocuticle (ex) and endocuticle (en). E) Cross section of the ScP vein (layering comparable to a longitudinal vein) with the cuticle being composed of five different layers: epicuticle (epi), exocuticle (ex), mesocuticle (me), second, thinner exocuticle (ex2) and endocuticle (en). Flexible membrane (mb) is attached to the vein. F) Cross section of a cross vein composed of three layers: epicuticle (epi), exocuticle (ex) and endocuticle (en). G) Cross section of a longitudinal vein with the cuticle being composed of the five usual layers plus an additional mixed layer (mi). AA—anal vein anterior, arc—arculus, CA—costal vein anterior, CP—costal vein posterior, CuA—cubital vein anterior, CuP—cubital vein posterior, dc—discoidal cell, epi—epicuticle, ex—exocuticle, ex2—exocuticle 2, fl—flexible, resilin-bearing joint, fu—fused joint, IR1—intercalated vein interradial sector 1, IR2—intercalated vein interradial sector 2, MA—median vein anterior, mb— membrane, M&Cu—mediocubital stem, MP—median vein posterior, Mspl—medial supplemental vein, RA—radial vein anterior, RP'—radial vein posterior (anterior branch of basal radial fork / midfork), RP''—radial vein posterior (posterior branch of basal radial fork/midfork) (= RP3/4), RP1—radial vein posterior (anterior branch of distal radial fork), RP2—radial vein posterior (posterior branch of distal radial fork), Rspl—radial supplemental vein, ScA—subcostal vein anterior, ScP—free subcostal vein posterior, sp—spine, ta—triangle, ps—pterostigma, tr—tracheal membrane. Scale bars: B) 50 µm, C) 20 µm, D) 1 µm, E,F) 10 µm, G) 5 µm.

of a single vein joint depends on the type of surrounding vein joints.[163]

A special joint in odonatan wings is the nodus. It is located at the leading edge, comprises costal and subcostal vein parts and divides the wing into a dorsally upwards facing pre-nodal leading edge and a downwards facing post-nodal leading edge. Through its specialized morphology with a dorsally often prominent elevated ridge, it creates a dorsoventral asymmetry, providing higher resistance to aerodynamic forces during the downstroke.[164] Resilin is present on both sides of the nodus but more prominent on the ventral side. Finite-element simulations showed that it increases translational and rotational displacements of the nodus, thereby enhancing lift generation arising from leading edge twisting,[126,165] and transmits the stress to the costal and radial veins, away from the thinner subcostal vein.[164] The more proximally such a flexible joint in the leading edge is located, the

higher is the torsion of the wing, with Diptera and their costal breaks representing an extreme example (e.g., review by Wootton in 2020).[116]

Resilin was not only found in dragonfly wing vein joints but also in the inner layers of dragonfly wing veins.[65] While the outer layer (exocuticle) of such veins is rather stiff and sclerotized, one of the inner layers, the endocuticle, was assumed to be rather soft and compliant due to a large proportion of a proteinous, resilin-bearing matrix (Figure 5D–G).[65] This stiffness gradient is especially pronounced in longitudinal veins, which significantly differ from cross veins in having a much thicker endocuticle than exocuticle (exceptions are the cross veins spanned between the costal and subcostal posterior veins).[65] Such a stiffness gradient was further suggested to 1) reduce the overall vein stiffness, 2) enhance elastic energy storage and 3) increase the load-bearing capacity against failure by Brazier ovalization.[65,166]

1.5. Alar Fenestrae, Flexibly Anchored Hamuli, Flexion and Fold Lines in Hymenoptera

In contrast to wings of dragonflies and other Palaeoptera, which have a rich and pronounced venation and corrugation along the whole wing, wings of Hymenoptera and some other orders of the Neuroptera show 1) a pronounced reduction of corrugation and the number of cross veins and 2) an increase of the relative membrane cell size. The longitudinal veins of Hymenoptera tend to end blindly in the distal wing area, thereby creating incompletely bordered distal cells.[167] In such wings with a reduced and incomplete vein network, the latter is not the main source for the wings' directional deformation during flight. Wing deformation is also directed by flexion along so-called flexion lines (not to be mixed up with the "flexion lines" in Odonata, which are based on the distribution of flexible vein joints),[61,158] which pass through wing membrane cells and wing veins and are independent from longitudinal-vein-to-cross-vein joints.[117,168] They can be perceived as more hyaline areas in the wing membrane and as transparent breaks within veins (so called *alar fenestrae*) and often contain a large proportion of resilin, which increases their flexibility and simultaneously prevents wear at these highly stressed regions (**Figure 6**A–C).[62,119,169] Through the sometimes asymmetrical distribution of resilin in the flexion lines on the dorsal and ventral wing sides, the flexion lines can endow the respective area with directional stiffness.[170] They allow the rotational movement of whole wing areas and thereby contribute to major wing shape changes in hymenopteran wings during flight. For example, they permit camber generation and reversal during downstroke and upstroke, respectively, and help control the angle of attack and the extent of deformation of the distal part of the wing.[117,168,171]

Wings of Hymenoptera show up to six different flexion lines in the forewing and a reduced set (of usually one or two) in the hindwing.[167–169,172] These include the following longitudinal flexion lines: 1) the median flexion line, 2) the radial flexion lines (anterior, posterior), 3,4) the medial flexion lines (anterior, posterior), and 5) the claval furrow (also named claval flexion line) (**Figures** 6A,C,**7**A).[167,169,172,173] Except for the median flexion line, which is convex with respect to the dorsal side of the wing, all other flexion lines in Hymenopteran wings are concave and, therefore, can be easily distinguished from the convex wing veins (Brackenbury claimed that the median flexion line is concave, but from his description, it can be deduced that he mixed up the median flexion line with the posterior radial flexion line.).[168,169,172,173]

The median flexion line runs posterior to the Sc+R vein and anterior to the median vein and sometimes crosses the radial vein branches (for all flexion lines, see Figures 6A,C and **7**A).[169,171,174] The radial flexion lines run between the medial and radial veins.[169] The medial flexion lines, which have also been denoted as medial folds, run posterior to the medial vein.[169,173,175] The claval furrow (or claval flexion line) is a nearly universal flexion line, which can be found at more or less the same position in the fore and hindwing and in different families of the Neoptera.[171] It normally lies between the posterior cubital vein (or M+Cu) and the first anal vein. It extends to the claval notch at the wing margin of the trailing edge, thereby separating the (posterior) remigium from the anal wing area.[168,171,174] During the downstroke, the wing is deflected in the claval flexion line to compensate for a shortening of the wing blade caused by the approaching medial (or M+Cu) and anal veins.[151] The latter is caused by the (1) contraction of the dorso-longitudinal muscles at the one hand (leading to a downwards directed movement of the anterior part of the wing, with the rotational movement of the first and secondary axillary sclerites being involved) and (2) contraction of the axillary lever muscle (having a decreasing effect on the wing pronation and causing the upper end of the third axillary sclerite and, therefore, also the base of the anal vein to move and tilt forward and down so that the leading edge rises to a higher level than the trailing edge).[151]

Apart from these more universal flexion lines, Ma and co-workers showed the existence of a resilin-dominated stripe on the ventral side of the area separating the costal vein and the Sc+R vein (In their publication, they wrongly denoted the costal and Sc+R veins as outer and inner sub-veins of the costal vein.) (Figures 6A,C,D and 7A).[176]

When flexion lines pass through wing veins, the latter often show an alar fenestra, a hyaline, resilin-containing break, at this region.[168,177] In hymenopteran wings, resilin usually is either only present at the dorsal side of the alar fenestra or can be found on both sides with the dorsal side showing a more pronounced resilin patch (Ma and co-workers most probably mixed up dorsal and ventral wing sides.) (Figures 6A–C and 7A,B,E).[177,178] Examples for veins showing alar fenestrae are 1) the two m-cu cross veins (1m-cu: one fenestra (Figures 6B and 7B); 2m-cu: two fenestrae; with the medial flexion lines passing through), 2) the 1cu-a (=cu-v) cross vein (Figure 7D) and the distal end of the Cu1b vein (=2CU[169]) (Each having one fenestra; with the claval flexion line passing through.), and 3) the second free abscissa of Rs (=2RS[169]) and both r-m cross veins (2RS: one fenestra; 1r-m: one fenestra; 2r-m: two fenestrae; with the radial flexion lines passing through) (Figures 6A–C and **7**A,B,E).[167,169,179] In contrast to the forewing of Hymenoptera, which often shows a full set of alar fenestrae, the hindwing usually only has one or two (the cu-a alar fenestra and the r-m alar fenestra) (Figure 7A).[167,178]

While in wings of Hymenoptera alar fenestrae are mainly found in cross veins, in wings of Ephemeroptera, such alar fenestrae are called "bullae" and are located at concave longitudinal veins (e.g., ScP, RP, MP), spanning a flexion line

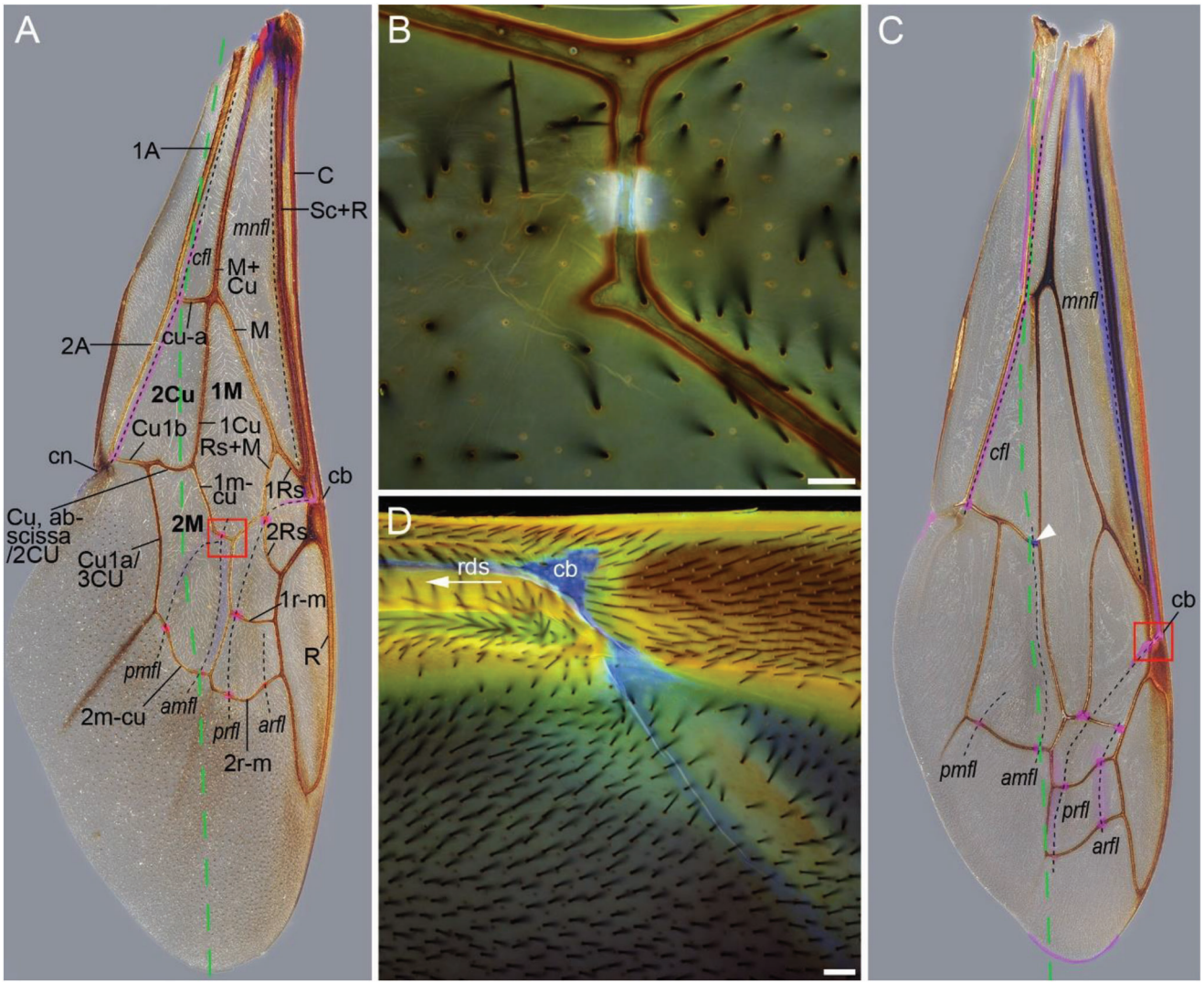

Figure 6. Occurrence of resilin in wings of bumble bees and wasps. A,C) Light microscopy. Blue, red, and pink coloration indicate the presence of resilin on the ventral, dorsal or both wing sides, respectively. Green, dashed line indicates the course of the fold line, type A. Black dashed lines show the course of flexion lines. B,D) Confocal laser scanning microscopy. A,B) *Bombus terrestris*. A) Left forewing, ventral view. B) Detail of red square in (A), 1 m-cu joint of the dorsal side of the left forewing. C,D) *Vespula vulgaris*. C) Left forewing, ventral view; white arrowhead—alar fenestra only present on the last abscissa/2CU vein of vespids. D) Detail of red square in (C), costal break (cb) at the leading edge and resilin-dominated stripe (rds) between C and Sc+R, left forewing, ventral view. 1A—first anal vein, 2A—second anal vein, *amfl*—anterior medial flexion line, *arfl*—anterior radial flexion line, C—costal vein/Costa, cb—costal break, *cfl*—claval furrow (claval flexion line), cn—claval notch, 1Cu—first cubital vein/Cubitus, 2Cu—second cubital cell, cu-a—cubito-anal cross vein, Cu1a/3CU—first cubital branch, Cu, abscissa/ 2CU—second cubital vein, Cu1b—second cubital branch, 1 M—first medial cell, 1m-cu—first medio-cubital cross vein, 2 M—second medial cell, 2m-cu—second medio-cubital cross vein, M—medial vein/Media, M+Cu—Media + Cubitus, *mnfl*—median flexion line, *pmfl*—posterior medial flexion line, *prfl*—posterior radial flexion line, 1r-m—first radio-medial cross vein, 2r-m—second radio-medial cross vein, R—radial vein/Radius, 1Rs—first radial sector, 2Rs—second radial sector, Rs+M—radial sector + Media, Sc+R—Subcosta + Radius. Scale bars: 50 µm (B, D).

along the wing chord in anterio-posterior direction and enabling a spanwise wing bending in ventral direction during wing supination.[116,180,181]

A study by Mountcastle and Combes showed that even the stiffening of a single resilin-bearing alar fenestra affects the flight performance of a bumblebee (*Bombus impatiens* Cresson, 1863).[177] They found a full set of the above-described alar fenestrae in the forewing and artificially stiffened one of the 1m-cu vein (called 1m-cu joint, (Figure 6A (red square), B)) of a living bumblebee with a microsplint glued across the joint with cyanoacrylate and examined the wing's flexural stiffness and the maximum vertical aerodynamic force production.[177] Their study showed that the stiffening of the 1m-cu joint causes a reduction in overall chordwise flexibility, thereby preventing concave camber formation in the wing during supination and transition into the upstroke.[177] They further found that bumblebees with stiffened 1m-cu joints produced less maximum vertical aerodynamic force and supposed that such a wing stiffening can negatively affect the

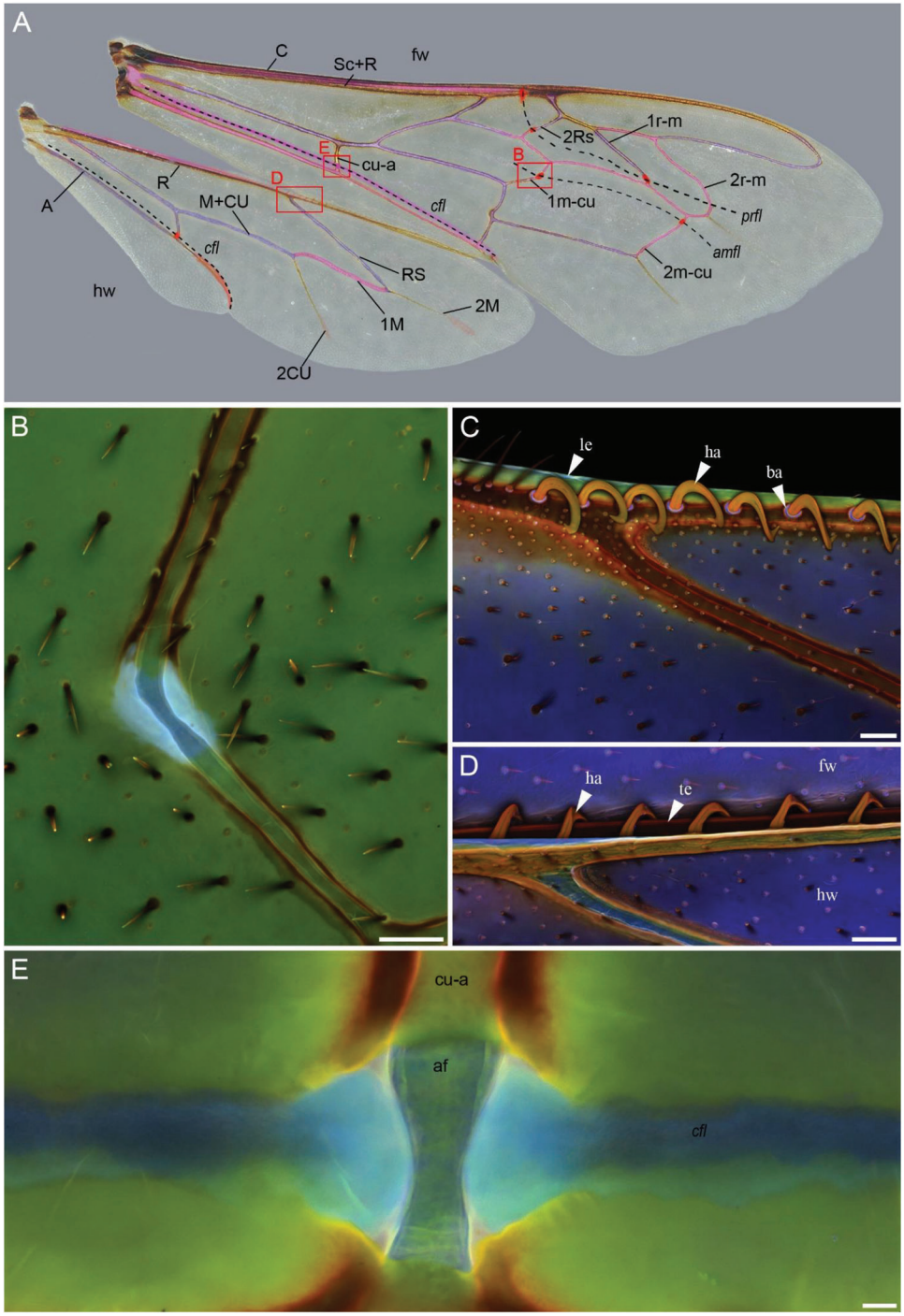

Figure 7. Occurrence of resilin in wings of the honey bee *Apis mellifera*. A) Light microscopy. Blue, red and pink coloration indicate the presence of resilin on the ventral, dorsal or both wing sides, respectively. B–E) Confocal laser scanning microscopy. A) Ventral side of the left forewing and hindwing with the leading edge of the hindwing being connected to the trailing edge of the forewing. B) Detail of red square in (A), 1 m-cu joint of the dorsal side of the left forewing. C) Distal hamuli (ha) with a flexible base (ba) at the leading edge (le) of the hindwing, dorsal side. D) Connection of the distal hamuli (ha) of the hindwing (hw) to the sclerotized trailing edge (te) of the forewing (fe), ventral view. E. Alar fenestra of cu-a with claval flexion line (*cfl*) passing through. af—alar fenestra, A—anal vein, *amfl*—anterior medial flexion line, ba—flexible base of the hamuli, C—costal vein/ Costa, *cfl*—claval furrow (claval flexion line), 2CU—second cubital vein, cu-a—cubito-anal cross vein, fw—forewing, ha—distal hamuli at the leading edge of the dorsal side of the hindwing, hw – hindwing, le—leading edge, 1m-cu—first medio-cubital cross vein, 2m-cu—second medio-cubital cross vein, 1 M—first medial vein/ Media, 2 M—second medial vein/ Media, M+Cu—Media + Cubitus, *prfl*—posterior radial flexion line, R—radial vein/ Radius, 1r-m—first radio-medial cross vein, 2r-m—second radio-medial cross vein, Rs—radial sector, 2Rs—second radial sector, Sc+R—Subcosta + Radius, te—trailing edge of the forewing. Scale bars: B–D) 50 μm, E) 10 μm.

production and/or maintenance of the leading edge vortex during supination and thereby decrease lift production.[177,182]

Ma and co-workers examined wings of the western honeybee (*Apis mellifera* Linnaeus, 1758) and found a reduced set of alar fenestrae in the forewing with the ones in 2r-m and the posterior one in 2m-cu lacking (Figure 7A, reviewed distribution of resilin).[178] As already assumed by Mountcastle and Combes, they supposed that resilin in the form of alar fenestrae and flexion lines in bumble bee wings can increase the wings' chordwise flexibility, support camber formation and, thereby, improve the aerodynamic performance.[177,178] Based on the distribution pattern of wing veins and resilin patches, the occurrence of a flexible hook-mediated forewing-hindwing-connection and recorded wing deformations, they further suggested the existence of five flexion lines in one forewing-hindwing entity.[178,183] These flexion lines or rather some parts of them can be interpreted as the claval flexion line (flexion line 1 and 3 in hindwing and forewing, respectively), the anterior medial flexion line (flexion line 4) and the posterior radial flexion line (flexion line 5), supplemented by the flexible forewing-hindwing-connection (flexion line 2) (numeration according to Ma et al. 2015) (Figure 7A).[178]

Besides their aerodynamic function, flexion lines or parts of them can also serve other purposes like mitigating collision damage when the wings hit an obstacle.[119] The reduction of wing fracture is very important because wing area loss reduces the load-lifting capacity, necessitates a higher wing beat frequency and increases the rate of mortality.[184,185] In this context, Mountcastle and Combes described another peculiarity of some hymenopteran wings, the costal break (also called costal notch).[119] It is a flexible, resilin-bearing joint or break in the leading edge, usually separating prestigma and stigma (Figure 6C (red square), D).[119] According to Danforth, it can be interpreted as part of the posterior radial flexion line and was observed to support flexion and twisting of the distal wing half during supination.[167,172] In order to test the role of the costal break in minimizing collision damage, Mountcastle and Combes rotated the wings of a yellow jacket wasp (*Vespula maculifrons* (Buysson 1905)) against the surface of a leaf.[119] They used wings with a splinted, immobilized costal break and unaltered ones and found that the immobilization of the costal break results in a drastically increased rate of wing wear (i.e., loss of wing tip area).[119] They further demonstrated that bumblebee wings (*Bombus impatiens* Cresson 1863), which do not have such a pronounced costal break, show less collision damage than the splinted yellowjacket wings and concluded that wing wear in bumblebees is rather reduced through the increased flexibility of the unreinforced wing tip than through a pronounced costal break.[119] The role of the spanwise vein tapering towards the tip in reducing the wing tip's moment of inertia and generated stresses and in increasing its flexibility was already discussed by Wootton in 1992.[115]

A study by Zhao and co-workers further showed for honeybee wings that wing stiffness and recovery time after wing deformation due to collision with an obstacle is probably not only affected by the wing's structure and material composition but also by hemolymph pressure in the wing veins (especially in leading edge veins like the subcostal vein), which increases wing stiffness and thereby reduces the recovery time.[186] Additionally, they assumed that hemolymph affects the wing's vibration characteristics by increasing the mass and the moments of inertia.[115,186]

Another character of the Hymenoptera and all other Neuroptera is their ability to flex and tightly abut their wings horizontally against their abdomen instead of simply position their outspread wings at the sides or over the abdomen like the Palaeoptera (with the exception of the Diaphanopterodea, which evolved a second mechanism to fold their wings horizontally over their abdomen).[187–190] Thereby, they are able to move faster through the vegetation to, e.g., escape predators, hide in small, narrow spaces and colonize new habitats.[191] In addition, many Neopterans are able to fold their wings along special fold lines of higher flexibility in fan-wise, transverse and/or longitudinal direction to create an origami-like wing package of much smaller dimension if compared to the unfolded wings.[191] Like flexion lines, fold lines are flexible and supplemented by resilin.[62] However, in contrast to most of the hymenopteran flexion lines, fold lines in wings of Hymenoptera tend to be convex with respect to the dorsal side of the wing.[168] Unlike flexion lines, which primarily serve aerodynamic functions, fold lines most of all serve wing folding.[171] To some extent, however, flexion lines can also contribute to wing folding, and fold lines can additionally support wing flexion during flight.[171] Based on the number and arrangement of fold lines, wing folding in Neoptera ranges from being quite simply (as in most Hymenoptera) to very complex (as in Dermaptera).[62,191] While Hymenoptera, some Lepidoptera and Trichoptera usually use only one wing folding mechanism (longitudinal folding), Coleoptera combine two folding mechanisms (transverse and longitudinal folding), and Dermaptera use a combination of all three folding types (transverse, longitudinal and fan-wise folding).[191] The mechanisms for wing folding and unfolding as well as the ones for stabilizing the folded or unfolded wing are quite diverse and include the involvement of different body parts, muscles, movements, the use of resilin's intrinsic elasticity, and structure-based click-mechanisms (see below).[168,191]

In most of the hymenopteran wings, a single, dorsally convex, longitudinal fold line is used to form a single plaiting fold with the ventral sides of the wing halves touching each other.[168] Danforth and Michener distinguished between two fold line types, namely plaiting fold A and B.[168] Plaiting fold A was shown to be present in wings of Vespidae, Eulonchopria, Gasteruptiidae, Figitinae and Leucospidae.[168] It runs from the posterior wing margin near the wing base across the anal vein (vannal vein) and the cu-a (cu-v) cross vein where it passes through the alar fenestra (Figures 6A,C and 8A,C).[168] It then runs across the second cubital cell, the last abscissa of Cu, through the medial cell and the anterior alar fenestra of the 2 m-cu cross vein and finally across the distal part of the medial vein (Figures 6A,C and 8A,C).[168] In wasps, an additional alar fenestra on the anterior part of the last abscissa of Cu (=2CU[169]) exists, which cannot be found in wasps that do not fold their wings (Figure 6C, white arrow).[168,169] Plaiting fold A is very pronounced and is only less acute at the base and the tip of the wing.[168] Variations between different families include the existence of additional or less alar fenestrae or diffuse vein weakenings, a slight alteration of the fold line's path through the respective veins and a varying acuteness of the fold line and degree of vein sclerotization.[168] Plaiting fold B is present in the wings of the pompilid genera *Episyron* and *Poecilopompus*.[168] It starts at the wing base anterior to the M+Cu vein and further continues parallel and very close to M+Cu, then passes through an

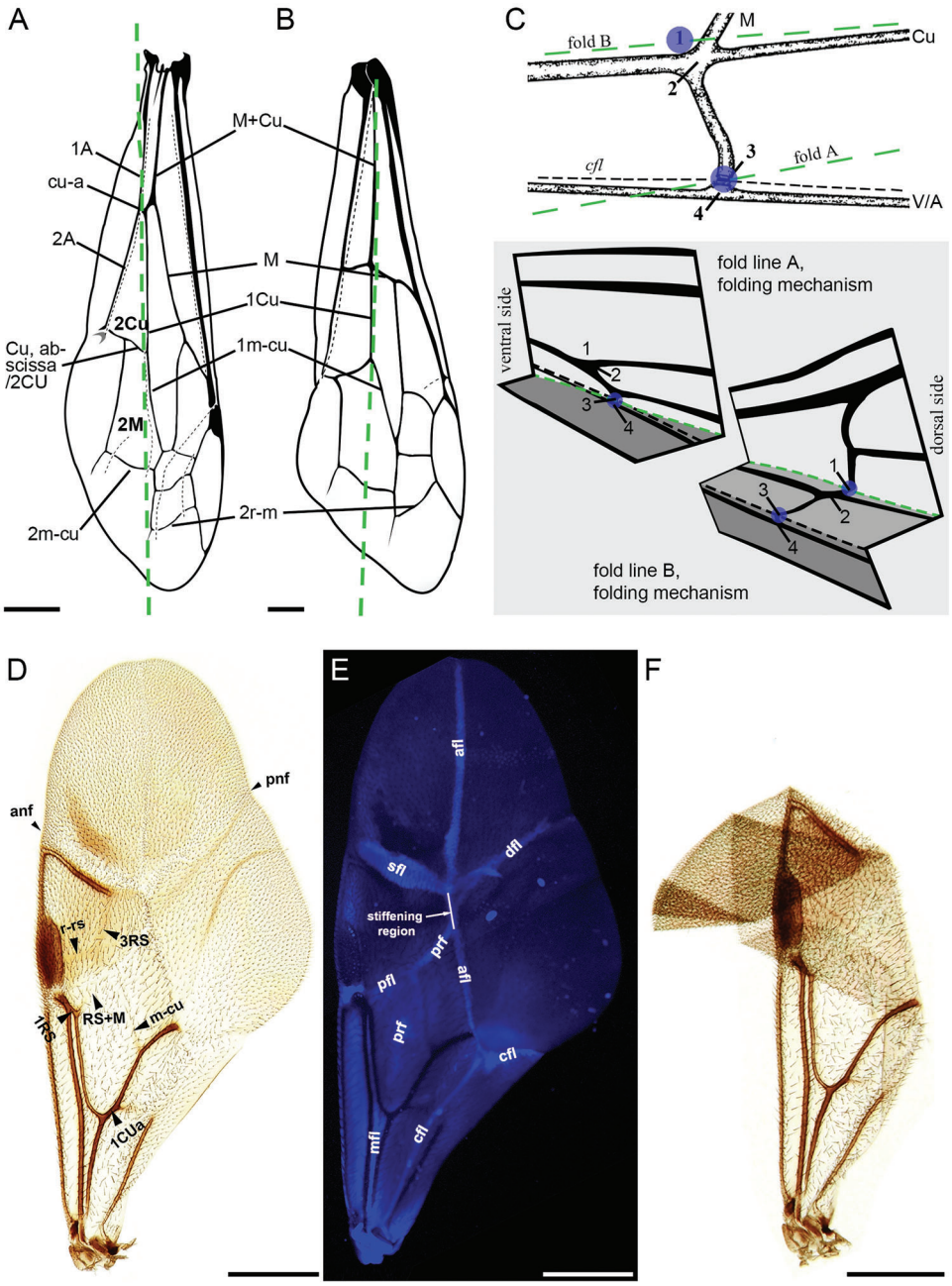

Figure 8. Folding line types and folding in ensign wasps. A–C) Wing schemata with green line indicating the fold line. D,F) Light microscopy. E) Confocal laser scanning microscopy. A–C) Course of folding and flexion lines according to data from.[168] B,C) Drawings of wing and veins based on a photograph kindly provided by the Smithsonian National Museum of Natural History, Department of Entomology. D–F) Reproduced with permission.[169] Copyright 2014, Public Library of Science. A) Forewing of *Vespula maculifrons*, showing a type A fold line. B) Forewing of *Poecilopompilus algidus*, showing a type B fold line. C) Enlarged schemata showing the alar fenestra of the cu-a cross vein in wasp or bee forewings with fold lines of type A and B (in reality, both fold lines never occur together in one species); grey box: folding mechanisms of fold lines of type A (normal folding) and B (zigzag folding), with blue dots indicating flexible areas and black dots indicating veins, mechanism shown in cross section. D–F) Forewing of *Afrevania longipetiolata* sp. nov. D,E) Fully unfolded forewing, showing flexion and fold lines. F) Folded forewing. 1A—first anal vein, 2A—second anal vein, *afl*—anal-marginal fold line, anf—anterodistal notch of the forewing, cfl—claval furrow (claval flexion line), Cu—cubital vein/ Cubitus, 1Cua (= 1Cu)—first cubital vein, 2Cu—second cubital cell, Cu, abscissa/ 2CU—second cubital vein, cu-a—cubito-anal cross vein, *dfl*—discal fold line, M—medial vein/ Media, 2 M—second medial cell, M+Cu—Media + Cubitus, m-cu (= 1m-cu)—first medio-cubital cross vein, 2m-cu—second medio-cubital cross vein, *mfl* = *mnfl*—median flexion line, *pfl*—prestigmal fold line, pnf—posterodistal notch of the forewing, *prf* = *prfl*—posterior radial flexion line, 2r-m—second radio-medial cross vein, r-rs—cross vein between radius and radial sector, 1Rs—first radial sector, 3Rs—third radial sector, Rs+M—radial sector + Media, *sfl*—poststigmal fold line. Scale bars: A,B) 1 mm, D–F) 500 µm.

alar fenestra at the medial (M) vein, then runs parallel to the cubital (Cu) vein, passes through the 1 m-cu vein at a less distinct vein weakening and finally passes through the medial cell and the 2 m-cu vein (**Figure 8**B,C).[168] Danforth and Michener further supposed that wings with the plaiting fold B can get another shape (z-shape) than wings with plaiting fold A when folded because the convex plaiting fold B and the concave claval furrow (claval flexion line) do not intersect (Figure 8C).[168]

Besides these usual longitudinal folds, some Hymenoptera have more curved fold lines, which are limited to special regions of the wing, like in the wings of the eucoilid genus *Kleidotoma*, which uses two curved fold lines in the distal part of the wing to wrap its wings over the metasoma.[168]

Mikó and co-workers further showed that hymenopteran wings also possess more complex wing folding mechanisms.[169] They reported on ensign wasps of the genera *Afrevania* and *Trissevania* that are able to fold their forewings along intersecting fold lines, a folding pattern comparable to the one used by some cockroaches.[169] Here, three intersecting fold lines, namely the anal-marginal fold line (afl), the discal fold line (dfl, which is probably derived from the posterior radial flexion line of other Evaniidae) and the poststigmal fold line (sfl, which is probably derived from the anterior radial flexion line) are used for the fourplane wing folding (Figure 8D–F).[169] Together with the anal-marginal fold line, the other two fold lines, namely the prestigmal fold line (which is probably derived from the stigmal break[169,192]) and the posterior radial fold line, seem to play a role in a locking mechanism, which is necessary for securing the unfolded wing position for flight (Figure 8D–F).[168,169]

In most of the hymenopterans that fold their wings along the type A fold line, the unfolded wing is prevented to fold up during flight by the so called click mechanism.[168,169] Usually, this mechanism involves wing regions where a concave and convex (flexion and/or folding) line intersect. An example is the alar fenestra of cu-a where the dorsally concave claval flexion line and the convex plaiting fold A converge (Figures 6A,C,7A,E, and 8A,C).[168,169] In the unfolded state, the alar fenestra is extremely concave, while it becomes strongly convex in the folded state.[168] Both positions are very stable and can only be inverted by alternating the configuration of cu-a.[168] Wing folding involves the intrinsic elasticity (energy storage) of resilin and the active flexion of the wing towards the longitudinal body axis, which (via the rotation of wing base sclerites) causes the M+Cu and anal veins to twist in opposite directions, leading to a reduction of the concavity at the alar fenestra and promoting convex plaiting.[168] Wing unfolding and stabilization of the unfolded state seems to be correlated with moving the wing to a position orthogonal to the body axis.[168]

As in wing folding, wing unfolding (as well as wing flexion and camber formation) can be additionally supported by the connection to the hindwings through hamuli.[122,168] Hamuli are hook-like setae, which are situated at the anterior margin of the leading edge of hymenopteran hindwings. Based on their morphology and the position along the leading edge, Basibuyuk and Quicke distinguished three classes of hamuli: the basal hamuli, the secondary ones and the distal ones.[193] Basal hamuli are apically flattened and generally curved towards the wing's tip but show some twisting after one third of their length.[193] They can be found clustered at the separation point of costa and subcosta on the hindwings of the members of three symphytan families (Xyleidae, Pamphiliidae, Xiphydriidae).[193] Secondary hamuli do not have the typical hook-like shape of basal and distal hamuli but are rather slightly bent and often show a bifurcated tip.[193] They are either dispersed along the proximal leading edge (in almost all Symphyta) or clustered beyond the separation point of the costa, subcostal and radius (in, e.g., Trigonalyoidea, Ichneumonoidea, Mutillidae, Bradynobaenidae, Rhopalosomatidae, Pompilidae).[191] Distal hamuli are present in all winged Hymenoptera and are normally found at the proximal end of the first radial vein in the distal wing half.[193] They are S-shaped and interlock with a strongly sclerotized ridge (also called recurved margin, frenal fold or retinaculum) at the posterior margin of the forewing's trailing edge (posterior rolled margin (PRM)) (Figure 7A,C,D).[193] The recurved margin's Archimedean spiral configuration, together with its thickened and sclerotized cuticle are assumed to improve the stability of the interlocking system by increasing the maximum coupling force the recurved margin is able to endure.[194] The surface of this ridge often features small protrusions, which provide additional grip for the hamuli.[195] The latter are sclerotized hooked structures and are embedded in a resilin-dominated membrane surrounded by a strongly sclerotized socket, which makes them flexibly suspended, comparable to insect mechanoreceptors (Figure 7C).[196] Their flexible, resilin-bearing bases and their rather stiff, hooked tips enable the hamuli to maintain a tight but flexible forewing-hindwing connection at alternating wing movements and forewing-hindwing tilt angles (allowing large angle variations of 135–235° between the wings), which is crucial for the wings' aerodynamic efficiency (especially by building a zone of ventral flexion (claval flexion line and connection line between forewing and hindwing) and thereby allowing strong camber reversal during the upstroke).[122,196–198] In addition, the movability of the hamuli allows certain lateral sliding along the ridge and was suggested to be advantageous for decoupling and re-coupling.[196] In this context, it is interesting that bees are able to re-couple their wings even in flight when they were uncoupled because of, e.g., contact to the vegetation (www.ibycter.wordpress.com/tag/hamuli/—video, leafcutter bee (Megachilidae)). Furthermore, the resilin-dominated membrane was suggested to increase the durability and reduce the risk of failure of the hamuli structures throughout a bee's lifetime.[196,198]

The number of distal hamuli varies widely within the Hymenoptera (ranging from two to over sixty), and sometimes differences in the number of distal hamuli occur even within one species and sometimes between the two hindwings of one individual.[193,199] Schwarz proposed that the number of hamuli can be related to body weight and (foraging) flight range, which is in agreement with the observation that the foraging flight range correlates with the number of hamuli in the alfalfa leafcutting bee *Megachile femorata* (Megachilidae).[199,200]

Apart from the wing plane, resilin has also been found in the wing base of Hymenoptera.[151] In the honey bee, it is present in the form of "resilin stripes" stretching between the basalare and the front edge of the humeral complex, where it is stretched during the upstroke, and between the third axillary sclerite (=pterale 3) and the anal vein as well as between the third axillary sclerite and the second axillary sclerite (=pterale 2).[151] In the latter case, Nachtigall and co-workers proposed that the resilin stripes might act as shock absorbers during the downstroke

when the sudden tilting movements of the second axillary sclerite are transmitted to the third axillary sclerite.[151]

1.6. Fold Lines in Earwigs and Beetles

In winged beetles and earwigs, forewings are thickened and sclerotized (elytra, beetles) or have a leathery appearance (tegmina, Dermaptera) and serve the protection of the membranous hindwings. In beetles, they were shown to not only protect against physical damage but also against diverse environmental challenges like desiccation, predation, and cold shock.[114] Hindwings are often meticulously folded into smaller wing packages to fit underneath the thickened forewings, thereby enabling the animals to hide in small crevices and to escape predators without damaging their hindwings.[191] In earwigs, the anciently long, stiff tegmina are further reduced in size, thereby increasing the movability of the abdomen, enabling its unhindered flexion in every direction and thereby facilitating crawling through narrow, twisted spaces. This adaptation requires an even more meticulous wing folding of higher packing ratio and leaves a sclerotized part of the wing, the squama, sticking out from under the tegmen. As mentioned above, wing folding occurs along flexible so-called fold lines. Based on the respective distribution and direction of these fold lines and additional flexible wing patches, coleopterans normally fold their wings in the longitudinal and transverse direction, whereas dermapterans show a more complex folding pattern with longitudinal, transverse and fanwise folding.[191]

1.6.1. Coleoptera

By examining Coleopteran hindwings (*Pachnoda marginata* (Drury, 1773) and *Coccinella septempunctata* Linnaeus, 1758) with fluorescence microscopy and high speed video recording, Haas and co-workers showed the existence of the following flexible fold lines: an anal fold line, a longitudinal fold line (which branches around the radial posterior vein in *P. marginata* hindwings) and one or two transverse folds (**Figure 9**A,C).[63,201] In addition, often shorter fold lines, which are folded or only briefly bent and re-flattened during wing folding, support the accurate execution of the folding process. The anal fold line runs along the anal anterior (AA or 1A). The longitudinal fold line is often located between RA and MP1+2 and partly runs along RP (in *P. marginata*, it branches in the middle of the wing and runs along RP2 and RP3+4&MP1+2). The first transverse fold runs from the leading to the trailing edge at around the middle of the wing and coincides with the distal end of RA (and MP1+2 in *C. septempunctata*) and the presence of the marginal joint (*P. marginata*). The second transverse fold line, if present, is located at the veinless wing tip (*C. septempunctata*). Most of the fold lines are convex with respect to the dorsal side of the wing, with the exception of the anterior longitudinal fold, the stiffening fold (which has also been denoted as a stiffening flexion line by Haas and co-workers) and some additional small fold lines.[63,201] The fold lines are supported by resilin on their ventral and dorsal sides at the proximal and center part of the wing and the leading edge (Figure 9A–D). Depending on its location, resilin can be suggested to help prevent material failure, to support wing deformations, and to assist wing unfolding. At the trailing edge and the wing tip, where the wing becomes thinner and thereby more flexible, the occurrence of resilin along the fold lines is less dominant.

Beetles normally fold their wings by brushing against them with their abdominal anisotropic microstructures in anterior direction and unfold them by using their thoracic muscles.[202,203] The overall folding process is comparable in all beetles.[204] When the wing is brushed towards the body, wing folding starts with the most proximal part of the wing being folded ventrally and the cubital (together with the media and radius posterior) veins moving closer to the radius anterior and the costa in the proximal part of the wing.[204] In the next step, the wing is transversely folded, bending the distal part of the wing ventrally, and the folding process often ends with additional folding of the wing tip.[202] However, despite different species have a comparable set of fold lines and fold their wings in an overall likewise manner, the details of the wing folding are quite diverse and lead to striking differences between the species not only in the shape and packing ratio of the folded wing but also in the distribution of resilin, here explained based on the two species *Coccinella septempunctata* Linnaeus, 1758 and *Pachnoda marginata* (Drury, 1773).[63,191,204–212]

In *C. septempunctata*, wing folding begins with a bending along the convex anal fold and another small concave fold present in this area (Figure 9A). At the same time, the wing is folded along the concave anterior longitudinal fold line and the concave stiffening fold line, enabling a deep folding and being supported by resilin-dominated cuticle (Figure 9A,B). The anterior longitudinal fold line is mainly folded along its proximal part, whereas it remains mostly flat in the distal part behind the first transverse fold, and concave folding is pursued along the stiffening fold line. This explains the lack of resilin along the distal part of the anterior longitudinal fold line, which is running posterior to the transverse fold line. In the further course, the distal wing half bends in ventro-proximal direction, thereby increasing the folding along the anterior longitudinal fold line and the stiffening fold and inducing the folding along the convex posterior longitudinal fold line. As a result of this, RP and RP2 are brought even closer to the leading edge joint, and the distal part of the wing is flipped over the leading edge so that its ventral side is facing up. During this process, the wing is folded along the convex first transverse fold line, thereby supporting the flipping movement. At the point where the first transverse fold line passes the radius posterior, the vein shows a flexible area comparable to the alar fenestrae of Hymenoptera. The wing is not only folded along the main fold lines but also briefly along some additional short fold lines at the leading edge (see examples in Figure 9A). In addition, Saito and co-workers proposed the existence of a diamond-shaped crease pattern comparable to that found in *P. marginata*.[212] Although the folding of this central part does not appear to have a great influence on the global folding, it can have an effect on the folding pattern of the stiffening fold and prevent material failure.[211] At the end, the wing is folded along the convex second transverse fold so that the folded wing obtains a zigzag shape. The function of the second alar-fenestra-like gap in the radius posterior becomes apparent when examining the fully folded wing, which is primarily folded in transverse direction along the first transverse flexion line and, in addition, slightly bent at this area (for wing folding in Coccinellidae, refer to, e.g., Haas and co-workers,[63] Saito and co-workers[211] (watch micro-CT animation), Song and

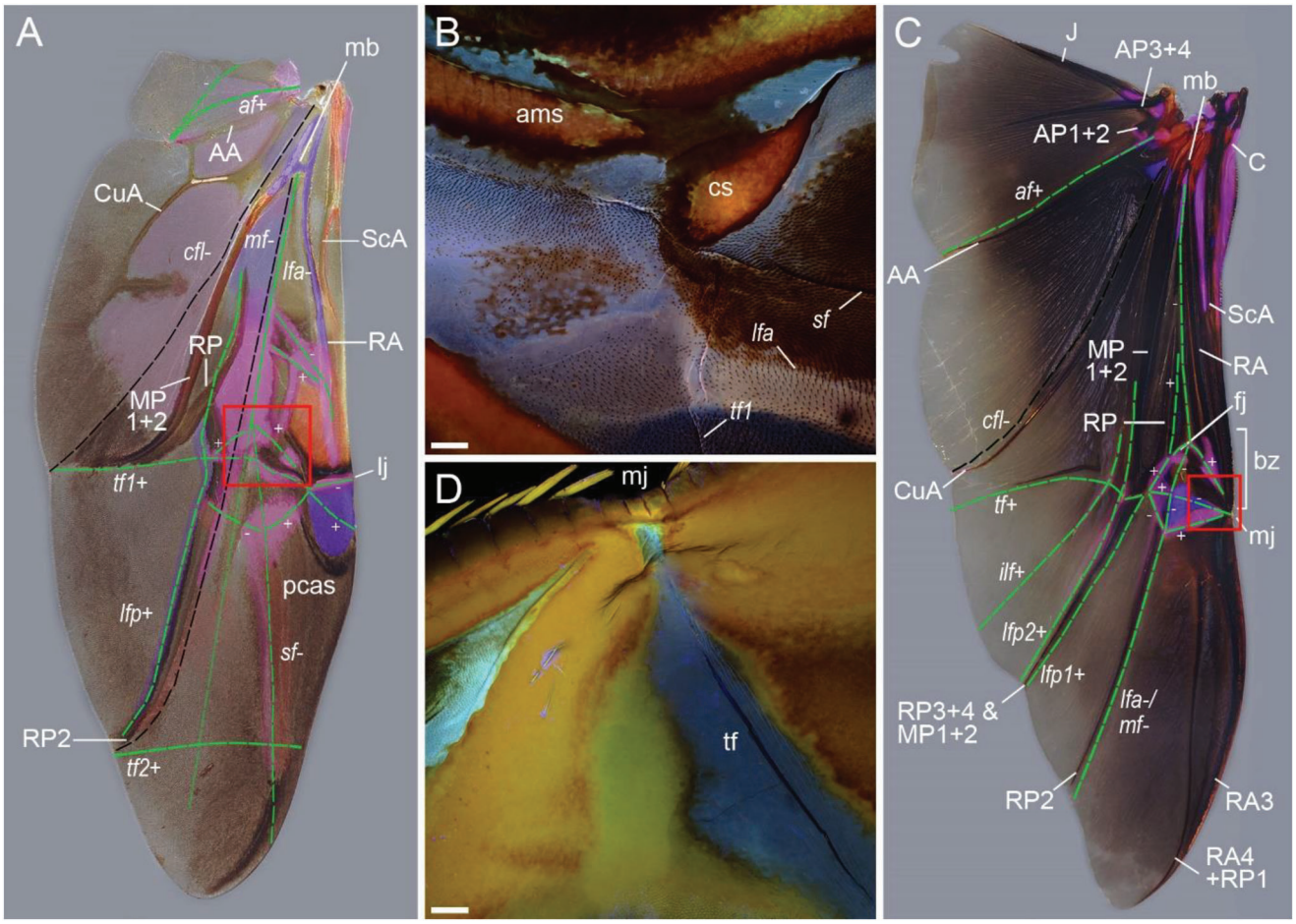

Figure 9. Occurrence of resilin in beetle wings. A,C) Light microscopy. B,D) Confocal laser scanning microscopy. A,B) *Coccinella septempunctata*. A) Left hindwing, ventral view. B) Detail of red square in (A), flexible folding zone with central sclerotization (cs) and anteromedian sclerotization (ams), stiffening fold line (sf), first transverse fold line (tf1) and shallow anterior longitudinal fold line (lfa). C,D) *Pachnoda marginata*. C) Left hindwing, ventral view. D) Detail of red square in (C), marginal joint (mj) with transverse fold line (*tf*). AA—anal anterior vein, *af*—anal fold line, ams—anteromedian sclerotization, AP1+2—first and second anal posterior vein, AP3+4—third and fourth anal posterior vein, bz—bending zone, C—costal vein/ Costa, *cfl*—claval flexion line, cs—central sclerotization, CuA—cubitus anterior vein, fj—flexible joint, *ilf*—intermediate longitudinal fold line, J—jugal vein, *lf*—longitudinal fold line, *lfa*—anterior longitudinal fold branch, *lfp*—posterior longitudinal fold branch, *lfp1*—first posterior longitudinal fold branch, *lfp2*—second posterior longitudinal fold branch, lj—leading edge joint, mb—medial bridge, *mf*—median flexion line, MP1+2—first and second media posterior vein, mj—marginal joint, pcas—postcosto-apical sclerotization, RA—radius anterior vein, RA3—third radius anterior vein, RA4 + RP1—fourth radius anterior and first radius posterior vein, RP—radius posterior vein, RP2—second radius posterior vein/branch, RP3+4 & MP1+2—third radius posterior and first and second media posterior vein, ScA—subcostal anterior vein, *sf*—stiffening fold, *tf*—transverse fold line, *tf1*—first transverse fold line, *tf2*—second transverse fold line. Scale bars: B,D) 100 µm.

co-workers[212]). Ladybird beetles unfold their wings before flapping, and, for this reason, unfolding of the wing was suggested to be driven by elastically stored energy in resilin-dominated areas and tape spring veins.[211,213,214]

Wing folding in *Pachnoda marginata* is driven by abdominal and elytral movement and begins with folding of the proximal part of the wing in ventral direction along the dorsally convex anal fold (Figure 9C). Subsequently, the wing folds along the concave anterior longitudinal fold (which runs along more or less the same path of the median flexion line). The RA and MP1+2 veins are moving against each other, with the medial bridge as pivot point and resilin at this proximal part avoiding material fatigue.[63] Haas and co-workers also suggest that the occurrence of resilin between the veins can be an indication for elastic energy storage taking place when RA, MP1+2 and CuA are approximated during wing folding.[63] The anterior longitudinal fold line further runs across a rather complex diamond-shaped fold field, which is dominated by resilin in those areas where fold lines are present (Figure 9C,D). At the same time, the convex fold lines (first and second posterior longitudinal fold lines) surrounding the RP, MP1+2 and RP3+4&MP1+2 vein area shift the latter dorsally so that the RP and MP1+2 veins come closer to the leading edge (RA) and now lie almost parallel to the RA vein.[63,203] In the further process, the distal wing half is folded in ventral direction along the convex transverse fold, which is running from the trailing edge up to the marginal joint. Where the transverse fold line crosses, RP3+4 and MP1+2 show a flexible articulation dominated by resilin on the dorsal and ventral wing sides

(comparable to an alar fenestra).[63,203] The more the wing is directed ventrally and downwards, the more the two convex proximal folds of the diamond-shaped fold field below the marginal joint are folded dorsally, thereby creating a small folding bag with the anterior longitudinal fold running through its center. Further folding along the anterior longitudinal fold establishes a close contact between the area of the diamond-shaped fold field lying above and the one lying below the anterior longitudinal fold. Together with the ventrally directed wing folding, this leads to folding in this upper part of the transverse fold, i.e., the part of the transverse fold that lies above the anterior longitudinal fold is folded in concave and the part lying just below the fold line is folded in convex direction. Finally, the two distal folds of the diamond-shaped fold field (see Figure 9D for the upper of the two distal folds), which are now lying on top of each other, are slightly folded in opposite direction to the part of the transverse fold that runs through the diamond-shaped fold field and their crossing point tugged in the ventrally concave fold of the MP1+2 and RP veins on the ventral wing side. As a result of this, the wing tip finally ends up lying under the CuA vein.[63,203] During this folding movement, the wrinkled bending zone is most probably stretched, bent and twisted, and its wrinkled structure helps avoid material failure.[63,215] In the course of the whole folding process, the wing is folded and flattened again along some rather indistinct fold lines in the trailing edge (one example is the (here termed) intermediate longitudinal fold line visible in Figure 9C).

In contrast to *C. septempunctata* wings, unfolding in *P. marginata* wings is probably directed by wing flapping and the scissor-like movement of RA and MP1+2 (and RP), thereby tightening the flexible joint between RP and RA as well as the diamond-shaped creases and the marginal joint and leading to an outstretched apical wing area.[63,191,213] Accordingly, wing unfolding is mainly driven by inertial and aerodynamic forces during fast flapping and to a minor part by direct thoracic muscular force but also by elastic energy storage during folding in the region of the marginal joint.[63,191,213]

During flight, the wing is bent along the concave flexion lines, i.e., the median flexion line, the claval flexion line and the stiffening flexion line, which is only present in *C. septempunctata* and has also been named stiffening fold because it plays a major role in wing folding (see above).[63] The median flexion line and the anterior longitudinal fold run along the same path and closely follow RP2 up to its end and can be regarded as one.[63,191,216] Therefore, in contrast to most other winged insects, in which the median flexion line is mainly essential for a proper wing deformation during flight, this flexion line also plays a role in the wing folding of the Coleoptera by being engaged in the angular separation/joining of RA and MP1+2.[191]

In contrast to wings of *P. marginata* and *Cyrtotrachelus buqueti* Guérin-Méneville, 1844, in which resilin can only be found at the intersection of the median flexion line with the anterior (marginal) joint, the median flexion line of *C. septempunctata* is accompanied by an enlarged resilin patch extending from its center up to its apical ending.[63] The claval flexion line either runs posterior to MP1+2 (*C. septempunctata* and *C. buqueti*) or posterior to CuA (*P. marginata*). As reported so far, it is not accompanied by a noticeable amount of resilin.[63,216] As already described above, the stiffening fold/flexion line runs anterior to the anterior longitudinal fold branch, starting from the centre of the longitudinal fold, rising to the anterior wing margin, running below the postcosto-apical sclerotization, thereby crossing the first and second transverse fold, and ending at the wing margin. Along its whole length, it is supported by resilin.[63] Meresman and Ribak showed that resilin- and structure-based wing compliance plays a role in increasing torque and causing camber and wing twist, thereby not only providing a higher flight efficiency and a higher maneuverability but also contributing to flight stability by decreasing the difference in wing pitch between the contralateral wings at turn initiation.[217]

As already mentioned before, wing flexion during flight takes also place at the fold lines (and the marginal joint in *P. marginata*).[63] Phan and Park examined the wings of free-flying rhinoceros beetles (*Allomyrina dichotoma* (Linnaeus, 1771)) under collision and found that under wing-tip collision, these wings often collapsed along the fold lines, thereby absorbing the collision forces, and returned to its outstretched form in less than 4 ms within a wing stroke.[213] While collisions without wing folding caused substantial changes in flight altitude, body posture and often lead to a tumbling flight, flight path and body posture were less perturbed in collisions with wing folding.[213]

1.6.2. Dermaptera

Earwig wings offer a conglomeration of joints, flexion and fold lines, veins, broadened vein patches and membrane areas supported by resilin on their dorsal and/or ventral sides (**Figure 10**A). The distribution of resilin mainly follows the pattern of wing folding, which is quite complex. While the leading edge, consisting of squama and apical fields, is stiff and tanned and only shows one flexible, resilin-dominated intermediate field, which is associated with wing folding, the ulnar field below the squama is less tanned and is interspersed with more flexible areas and lines (Figure 10A,B). The remaining part of the wing is membranous and more flexible, with several fold lines, flexible vein patches and veins as well as alar fenestrae, all of them enabling the specialized fan-wise, longitudinal and transverse wing folding.[62,218] Interestingly, the radiating (anal) veins at the distal membranous wing part are more sclerotized and thicker than most of the veins in the proximal part (except for the most proximal wing veins).[62,219] Veins at the proximal membranous part are often less sclerotized and thinner, dominated by resilin and flatten out towards the trailing edge (Figure 10A).[62,219] Deiters and coworkers assumed that the increased sclerotization and vein thickness in the distal part of the wing, together with the partial fusion of the second to fifth radiating (anal) veins, can help stabilize the wing and withstand strong bending forces and deformations during flapping flight.[219]

Wing folding in earwigs is not only special because of its complex folding pattern but also because of its mechanism. While beetles often actively fold and unfold their wings, earwig wings are only actively unfolded, but they are folded exclusively passively by the intrinsic elasticity of flexible, resilin-bearing wing vein patches and fold lines.[63,191,218,221] As in Hymenoptera, regular fold lines in earwig wings are convex with respect to the dorsal wing side. Nevertheless, due to the fanwise folding, the

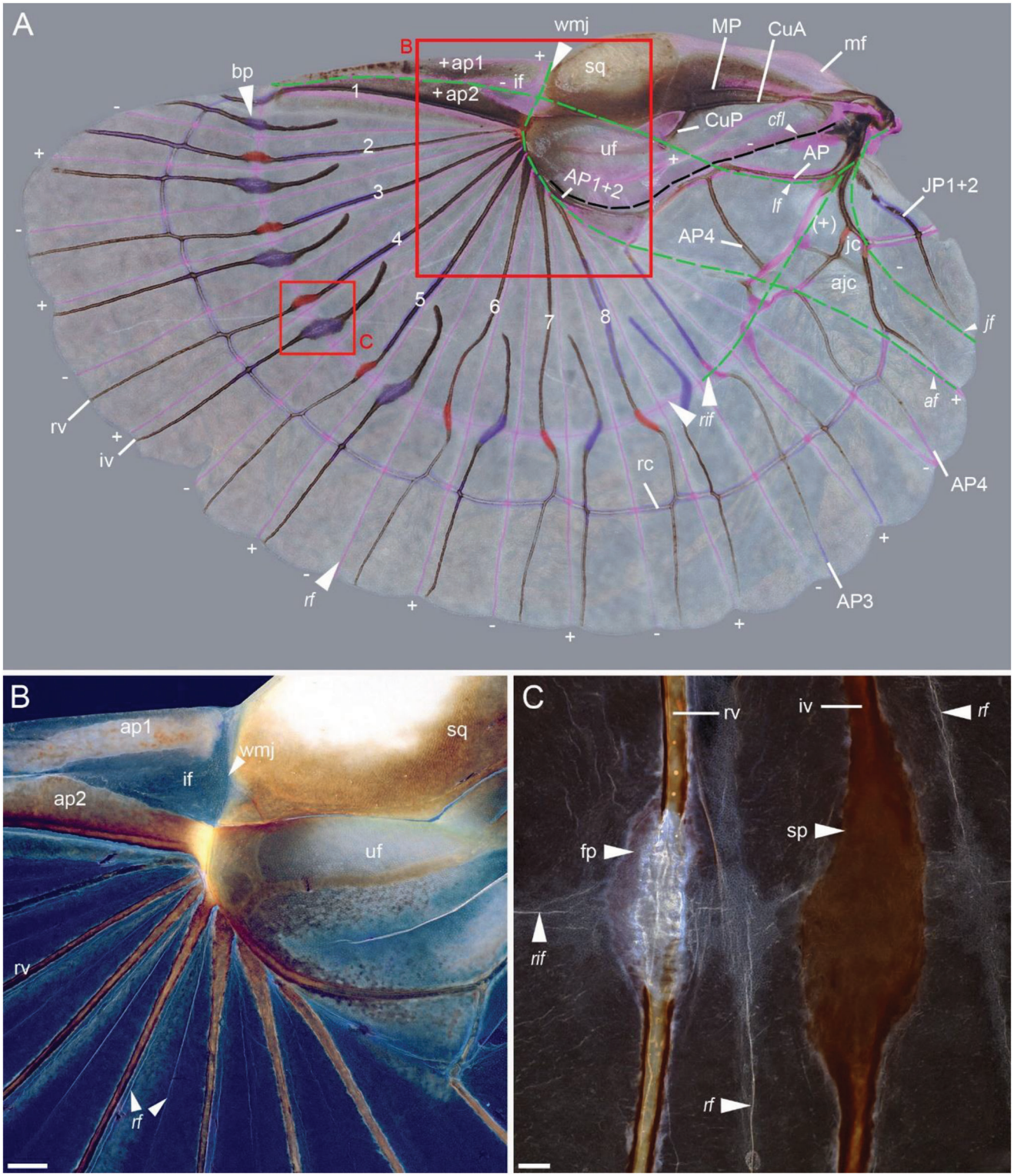

Figure 10. Occurrence of resilin in wings of the earwig *Forficula auricularia*. A) Light microscopy. B) Confocal laser scanning microscopy. A) Dorsal side of the left hindwing; dashed green lines indicate fold lines; except for the proximal part of the ring fold line, ring (*rif*) and radiating (*rf*) fold lines are not traced with dashed green lines for keeping the visibility of the resilin distribution. B) Detail of the larger red square in (A), showing the contact area of radiating veins (rv) with the ulnar field as well as flexible regions like the wing medium joint (wmj) with the intermediate/ central field (if) or radiating fold lines (*rf*). C) Detail of the smaller red square in (A), showing a dorsally flexible broadened vein patch (fp) of a radiating vein (rv) and a dorsally sclerotized broadened vein patch (sp) of an intercalary vein (iv), dorsal side of the left hindwing. ajc—anojugal cell, af—anal fold line (first transverse fold line), AP—anal posterior, ap1—outer apical area, AP1+2—first and second anal posterior, ap2—inner apical area, AP3—third anal posterior, AP4—

involved radiating fold lines alternately change in orientation (Figure 10A). All fold lines are dominated by resilin on their dorsal and ventral sides (Figure 10A). Where the radiating fold lines cross veins (i.e., ring cross veins), the veins show a reduced form of the alar fenestra known from wings of Hymenoptera, with resilin present on their dorsal and ventral sides. During the folding process, the dorsally alternating convex (+) and concave (−) radiating fold lines are pushed together fan-wise (Figure 10A–C).[62,218] Subsequently, the wing package is folded along the ring fold line (=second transverse fold line) in ventral direction with the fold line crossing the broadened vein patches.[62] Broadened vein patches of radiating (anal) veins are dominated by resilin on the dorsal side and more sclerotized on the ventral side (Figure 10A,C).[62] The same is true for the broadened vein patches of the intercalary veins, only the other way around. As a result, during wing folding, the resilin-dominated side of the broadened vein patches of radiating and intercalary veins is pressed together and forms an acute angle (concave), i.e., radiating vein patches bend to the dorsal side, while intercalary vein patches bend to the ventral side.[62] This automatic mechanism can be explained by the elastic recoil of resilin, which is stretched (in a stressed state) when the wing is completely unfolded and returns to its relaxed state during wing folding. After fan-wise folding, the wing is transversely folded along the convex anal fold (=first transverse fold).[62] Where the radiating (anal) veins meet the ulnar field, they are separated from the latter by a small ridge, which is part of the anal fold line and partially supported by resilin (see also Haas and co-workers[62]). On the dorsal side, the fourth radiating (anal) vein is connected to the inner apical area (Figure 10B), whereas on the ventral side, the second radiating vein meets the inner apical area.[62] Fusion of the third, fourth, and fifth radiating veins on the ventral side serve the coordinated folding and unfolding of the radiating veins.[62] Finally, the wing is longitudinally folded in ventral direction along the convex longitudinal fold line, which separates the squama and the ulnar field (Figure 10A–C).[222] The last step also includes folding along a short concave fold line, here termed the jugal fold line, running from the trailing edge to the wing base, where it meets the longitudinal and ring fold lines (Figure 10A). At the end, the wing area is reduced to 10% and sometimes even 5.5% of its size in the unfolded state and tightly packed under the tegmen, with only the squama being visible.[222,223]

Wing unfolding is either directed by cerci movements (e.g., *Forficula auricularia* Linnaeus, 1758; *Labia minor* (Linnaeus, 1758)) or by wing flapping driven by thoracic musculature and transmitted by the wing articulation (e.g., *Auchenomus* sp.; *Timomenus lugens* (Bormans, 1894)).[63,191,221] The latter mechanism especially occurs in earwigs with very long cerci that reach or even surpass the abdominal length.[221] What is striking about the wing unfolding are the bistable self-locking mechanisms, which inhibit the wing from folding during flight and work as a combination of fold and flexion lines and material gradients.[62,218,219,222,224] There are two of such mechanisms in the earwig wing, the mid-wing-mechanism and the claval flexion line.[62,218,219] The mid-wing-mechanism involves the intermediate (or central) field as well as the twofold lines, i.e., the anal fold line and the longitudinal fold line, which cross at the field.[62,218,219] It was described as bistable, basic mechanism, consisting of four plates (squama, ulnar field, outer and inner apical area), which are separated by four lines, i.e., the two crossing fold lines mentioned above (Figure 10A,B).[62,218] Because the total of the four angles around the crossing point are less than 360° (i.e., 350°), increasing of the opening angle between two basal plates beyond 180° leads to a sudden snap into the other of the two stable positions. When the wings are unfolded by the cerci or by flapping and the angle between the squama and the ulnar field (or between the two latter and the apical fields) rises above 180° by these movements, the wing is locked in this second stable position, comparable to a switch.[62,218] Resilin can be found on the ventral and dorsal sides of the involved fold lines and the intermediate field and was supposed to serve not only energy storage but also the prevention of material fatigue.[62] In addition, the compliant, resilin-bearing rhombic intermediate field was found to reduce the forces needed to change between the two stable positions, thereby alleviating the risk of failure as a result of high stresses.[62] Apart from its function in wing folding, the intermediate field, together with the anal fold line (which here acts as a flexion line), also play a role during flight by allowing the distal (outer) part of the wing to move differently from the squama and thereby supporting camber formation.[219] More precisely, during the downstroke, the distal wing part is bent upwards, thereby flattening the angle in the intermediate field and showing a more flattened (slightly concave) shape, whereas during the upstroke, when the distal part of the wing is bent downwards, the angle becomes more convex.[219] The double function as fold and flexion line with concave and convex bending can be a reason for the occurrence of resilin on the ventral and dorsal sides of the fold line.

The second mechanism for inhibiting accidental wing folding during flight involves the concave claval flexion line, which is also supported by resilin on both sides (Figure 10A).[62,218,219] It runs from the wing base across the ulnar field and along the anal posterior vein, thereby crossing the convex longitudinal fold line, which runs across the ulnar field and separates the latter from the squama. When the wing is folded along the longitudinal fold line, the claval flexion line is rather flat, but as soon as the wing is unfolded, the claval flexion line snaps into its concave form, rendering the ulnar field stable and stiff and preventing the convex folding or bending of the longitudinal fold line.[62] During the upstroke, when the distal wing part is bent downwards, the stiffening mechanism of the claval flexion line not only prevents the longitudinal fold line from becoming convex but also inhibits folding of the anal fold line by pushing it in through the stiffening of the ulnar field.[219]

fourth anal posterior, bp – broadened vein patch, *cfl*—claval flexion line/ claval furrow, CuA—cubitus anterior, CuP—cubitus posterior, fp—flexible side of a broadened vein patch, if—intermediate/ central field, iv—intercalary vein, jc—jugal cell, *jf*—jugal fold line, JP1+2—first and second jugal posterior, *lf*—longitudinal fold line, mf—marginal field (costal area), MP—media posterior, rc—ring cross vein, *rf*—radiating fold line, *rif*—ring fold line (second transverse fold line), rv—radiating (anal) vein/ branch (numbered from 1 to 8), sp—sclerotized side of a broadened vein patch, sq—squama, uf—ulnar field, wmj—wing medium joint. Scale bar: B,C) 50 µm. Nomenclature after.[218,220]

1.7. Membranous Resilin Patches and Halteres in Diptera

Flies are not only functionally two-winged fliers as hymenopterans or lepidopterans. Their hindwings have been transformed into a pair of mechanosensory halteres so that only the forewings are left to serve lift production during flight. Halteres are specialized gyroscopic organs and are used to control body rotation and to influence wing-steering muscles and head movements during flight.[225–227] In some families, they also have some functions during walking.[226,228] While other insect orders use their wings or, e.g., antenna for additional haltere-like functions, the morphology and material composition of dipteran halteres are specifically adapted to such functions.[229–231] Both, wings and halteres, contain resilin, and the hitherto existing knowledge of the distribution and function of resilin in these structures is described in the following paragraphs.

As in wings of Hymenoptera, dipteran forewings show flexion and fold lines, however, the exact positions of these lines have not been examined in detail until now. Wootton examined the wings of a hoverfly and assumed that dipteran forewings normally have two flexion lines (i.e., the median flexion line and the claval flexion line) and one fold line (i.e., the jugal fold).[171] In contrast to hymenopteran wings, in which the median flexion line lies between the Sc+R and M+Cu veins, this median flexion line is supposed to be located below the media vein (M) and above the first branch of the cubitus (CuA1) in Diptera (Figures 6A,C and **11**A). In Hymenoptera, the claval flexion line lies above the anal vein and below the M+Cu vein (Figure 6A,C). For Diptera, Wootton described that a flexion line, whose function is comparable to that of the claval flexion line in other insects and which, therefore, is further termed as such (by Wootton in 1979), lies below the first branch of the anal vein (A1), which is often fused with the second branch of the cubitus (A1+CuA2) (Figure 10A,C).[171] Autofluorescence analyses of the claval flexion line showed a narrow line of blue autofluorescence running posterior to CuP and A1+CuA2 and ending in a broader patch of blue autofluorescence anterior to A2 (**Figure 11**A,C). For most of the length of the suggested median flexion line, autofluorescence analyses do not show much proof of the existence of resilin autofluorescence, except for the part located in the basal medial cell, where it can be recognized as a relatively blurry line (Figure 11A,C). Nevertheless, the results indicate the presence of a 1) flexion line anterior to CuA1 and 2) one between the veins R4+5 and M, together with 3) a ventrally existing rudiment of an alar fenestra at the radio-medial cross vein, 4) a flexion line running across the squama in anterior-posterior direction and (5) a more flexible part of the media and the discal-medial-cubital cross vein (Figure 11A,C). The jugal fold, which is convex and accompanied by resilin, separates the alula, which is a part of the claval region of most brachycera flies and whose state was supposed to indicate different flight modes, from the alar squama, which represents the jugum in dipteran wings.[171,232,233]

In addition to the presence of resilin in flexion and fold lines, dipteran wings show highly distinctive resilin patches in close proximity to wing veins in the proximal part of the wing on the ventral and dorsal wing sides.[236] Such resilin patches have not been found in wings of other insect orders so far. Interestingly, they are lacking at the distal part of the wing, where the vein network is less dense (Lehmann et al. 2011).[236] Analyses of the wing's autofluorescence composition show that there is a material gradient, with the wing membrane being more flexible in the proximal part than in the distal part (Figure 11A–C). As reported by Lehmann and co-workers, bending moments are maximum near the wing root at the beginning of each half stroke (acceleration phase), when inertial forces peak.[236] Therefore, regardless of the elevated flexural stiffness of this wing area, local deflection is high.[236,237] Depending on the forces acting on the wing during the flapping cycle, the veins are either pressed together or pulled apart.[236] A mechanism for camber formation through the arculus, translating the upwards movement of the media to a twisting of the radius and the cubitus and thereby producing a downward movement of the trailing edge, was described by Ennos in 1989.[120,238] Such movements lead to a decrease or increase in membrane tension and possibly result in a stress-stiffening effect by the membranes (through transverse stiffening).[118,208,236,239] Resilin patches in these membrane areas were assumed to reduce material failure and peak stress.[236,237] High-speed video analyses of free-flying Diptera furthermore revealed the existence of transverse anterio-posterior running flexion lines, which bend the wings downwards at the end of the downstroke.[238] These transverse flexion lines exactly match the distribution of resilin patches (Figure 11A,B).

Despite the small bending moments near the wing tip, local deflection is also high in this wing part due to its lower flexural stiffness.[236] The lower flexural stiffness and higher compliance of the wing tip are probably due to the less dense vein network and decreased vein and membrane thickness and might serve the decrease of material failure when the wing hits an obstacle.[115,236] More flexible veins like the distal part of the media and the discal-medial-cubital cross vein might serve the same purpose.

At the costal leading edge, dipteran wings show breaks (less frequent/prominent in, e.g., lower Brachycera), i.e., the costa-gial/costal break, the humeral break and the subcostal break, whose location was supposed to be affected by pupal folds (Figure 11A,C).[238] These breaks are supplemented by resilin and are roughly comparable in function to the costal break in wasp wings, though they are often less prominent in shape (see above). In contrast to the costal break in Hymenoptera, the costal and humeral break in Diptera are unusually proximally located so that wing torsion can be quite extreme.[116]

By studying pro-resilin mutants as well as flies with mutated Rebers and Riddiford chitin-binding domain, Lerch and co-workers showed that flies without pro-resilin or chitin-binding domain were unable to fly and showed the held-down wing (*hdw*) phenotype, leading to the assumption that resilin in the wing base is crucial for wing flapping and holding.[46]

Small resilin-bearing structures can additionally be found at the tegula, near the wing base at the radial vein (or ScP+R vein), near or at the humeral cross vein, the radio-medial cross vein and the distal part of the first branch of the radius and along the radial branch anterior to the radio-medial cross vein, and they are attributed to the presence of campaniform sensilla (Figure 11C,D).[234,240–243] Campaniform sensilla are stretch-sensitive sensors and typically occur at sites of maximum strain.[231,234,241,244] They consist of a cuticular cap or dome, which is assumed to contain resilin in its second layer, and a sensory dendrite, which is connected to the cap by the tip of its sensory process.[240,245] When the wing cuticle is deformed, the cap is

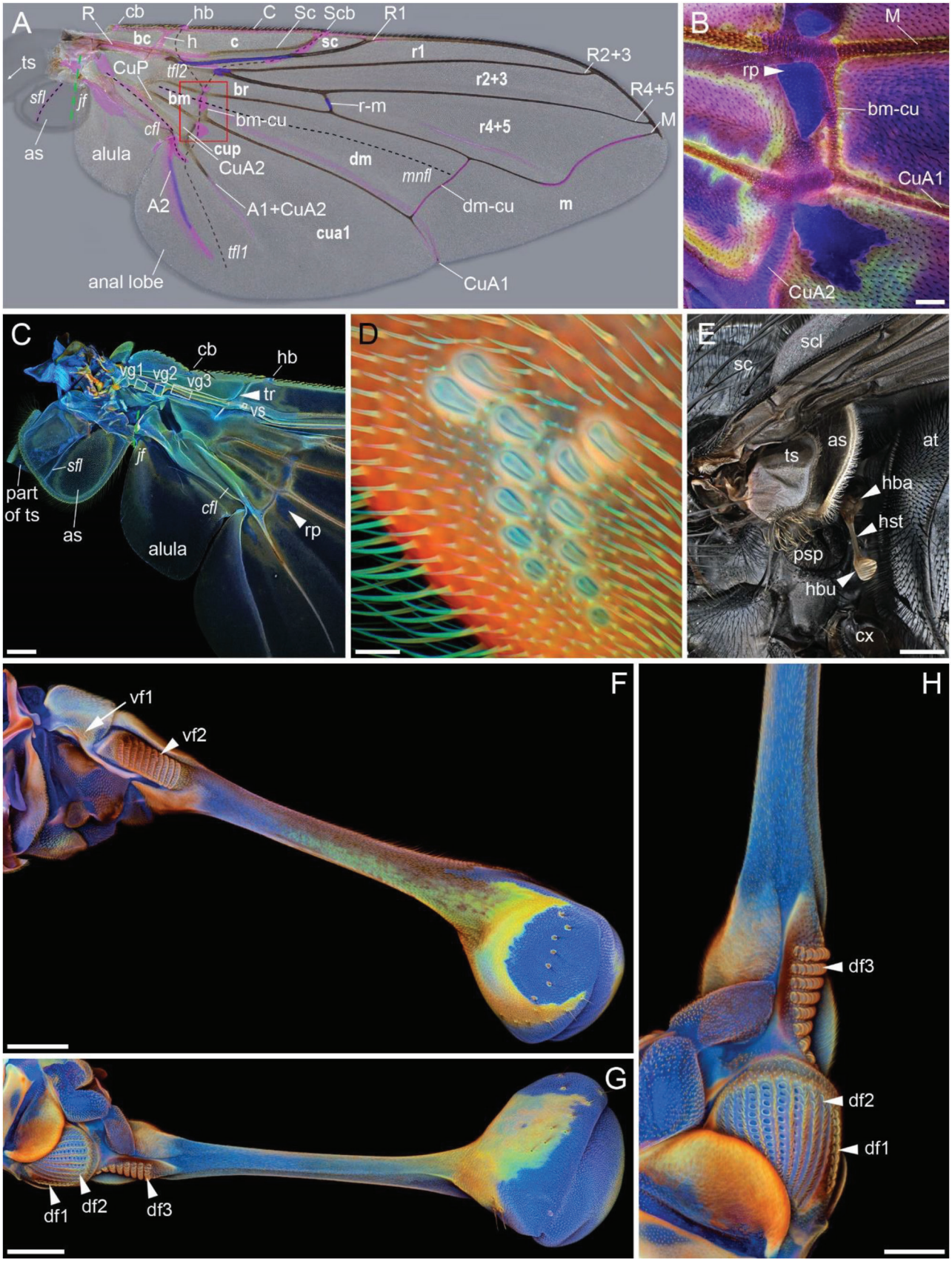

directionally deformed as well, transmitting the force to the sensory process of the dendrite, from where the signal propagates and innervates the B1 motoneuron, thereby providing feedback to and activating the first basalar muscle, which is an important steering muscle.[227,231,246] Resilin in the cap was supposed to allow the cap to resume its original form and can probably also serve fracture-resistance and as a flexible suspension for the sensory process.[245]

Campaniform sensilla were not only found in the wing but also on the bases of halteres in the form of sensilla groups and fields (Figure 11E–H).[226,234,241] Halteres are dumbbell-shaped appendages of the metathorax and consist of 1) a base, equipped with plates of mostly oval-shaped campaniform sensilla at the ventral and dorsal sides as well as Hicks papillae and chordotonal organs, 2) a slender stalk, which is more prominent in ancient dipteran families and shorter in more derived ones, and 3) an asymmetric bulb or end-knob, which is filled with prominent vacuolar cells, keeping the bulb cuticle constantly strained (Figure 11E–H).[244]

General autofluorescence analyses showed that halteres are more flexible at their tip than at their base.[247] The results of more detailed analyses reveal that the bulb generally consists of a homogenous flexible material, which is less flexible at the transition zone between the haltere stalk and head and at its posterior side where the bulb overhangs (Figure 11F,G). The posterior side of the stalk shows a comparable stiffness distribution towards its posterior side. The asymmetric form of the haltere bulb leads to a shift in the center of gravity to the rear axis of the haltere stalk and can explain the stiffer material present at this side.[244] Although the haltere base is relatively stiff in comparison to the stalk and bulb, the haltere hinge and the cap-like structures of the campaniform sensilla are more flexible (Figure 11F–H).[240,245,248,249]

Halteres typically oscillate at the same frequency as the forewings but at more or less the opposite phase (true only for Brachycera: 138–182°; in the more ancient Nematocera: wide variations from 0 to 211°).[228] This oscillation pattern is coordinated by the subepidermal ridge, a mechanical wing-haltere linkage in the thorax.[226,244,250] During flight, halteres experience large inertial and significantly smaller aerodynamical forces, and during body rotation, they are subjected to the angular velocity-dependent Coriolis force.[251] All of these forces cause torsion and bending of the stalk, thereby deforming the campaniform sensilla so that halteres can act as gyroscopes.[226,244,252] Therefore, in contrast to the wings' campaniform sensilla, which encodes chordwise and spanwise wing bending and thereby changes in aerodynamic and inertial forces acting on the wings,[227,253,254] i.e., forces that are more repetitive or phase-constant, campaniform sensilla on the bases of halteres deliver, apart from the more repetitive inertial forces, also rather quickly varying signals (Coriolis forces associated with body rotations), thereby additionally helping to counteract perturbations by influencing wing and head movements.[225–227] Because campaniform sensilla of one group or field often have a similar orientation, they are assumed to have a certain directional selectivity.[226,244] Further studies showed that campaniform sensilla of different fields (and also of different intra-field locations) deliver position-specific signal projections to specific locations in the thoracic ganglion.[246,255] For example, inputs from campaniform sensilla fields (probably on the radial vein) in the wings and inputs from predominantly those in the field dF2 of the halteres as well as from the compound eyes are integrated by the motoneuron MN.b1, having an effect on the generation of the typical phase-locked single spike of the basalar muscle during each wingbeat cycle, which can, however, dynamically change in its phase-value depending on the incoming signals from the visual and proprioceptive circuitry.[227,246,256]

2. Conclusions

In the insect flight system, resilin occurs in a variety of different structures, ranging from tendons of nearly pure resilin to delicate flexion and fold lines, vein breaks like costal breaks and alar fenestrae, internal layers of wing veins, longitudinal-to-cross-vein joints, wing membrane (patches), halteres, the flexible bases of mechanoreceptors (hair and campaniform sensilla) and hamuli to specialized structures like the prealar arm (peg) and the wing hinge as well as membranes connecting wing sclerites at the wing base.

According to its location and connection to other cuticle structures, resilin not only increases, e.g., the flexibility, adaptability, elastic energy storage, stress reduction, and failure resistance of the respective structure at its exact position, but often even tiny

Figure 11. Occurrence of resilin in the wings of the blow flies A–C,E,F) *Calliphora vicina*; D,G,H) *C. vomitoria*). A,E) Light microscopy. B–D, F–H) Confocal laser scanning microscopy. A) Left forewing, ventral view. Blue, red, and pink coloration indicate the presence of resilin on the ventral, dorsal or both wing sides, respectively. Green dashed line indicates the course of the jugal fold line. Black dashed lines show the course of flexion lines. For clarity reasons, upper (alar squama, as) and lower calypter (thoracic squama, ts) on the wing base were removed during preparation and are indicated as grey silhouettes. B) Detail of red square in (A), patches of resilin in the wing membrane. C) Wing base, left forewing, ventral side. White squares—groups of campaniform sensilla (vg1, vg2, vg3) and single campaniform sensilla (versus), visible at magnification. D) Group of campaniform sensilla, located at the forewing base, ventral side, detail of vg1 indicated in (C). E) Haltere at the left side of the metathorax, dorsal side of haltere visible. F) Haltere, ventral view, two campaniform sensilla fields (vf1, vf2) visible. G) Haltere, dorsal view, three campaniform sensilla fields (df1, df2, df3) visible. H) Detailed view of the three sensilla fields shown in (G). A1+CuA2—anal-anterior-cubitus branch, A2—second branch of the anal vein, as—alar squama, at—abdominal tergite, bc—basal costal cell, bm—basal medial cell, br—basal radial cell, C—costa, c—costal cell, cb—costagial/ costal break, *cfl*—claval flexion line, CuA1—first branch of cubitus, cua1—anterior cubital cell, CuA2—second branch of cubitus, CuP—posterior branch of cubitus, cup—posterior cubital cell, cx—coxa (third leg), df1–3—first, second and third dorsal field of haltere campaniform sensilla, dm—discal-medial cell, dm-cu—discal-medial-cubital cross vein, ds—dorsal single haltere sensilla, h—humeral cross vein, hb—humeral break, hba—haltere base, hbu—haltere bulb, hst—haltere stalk, *jf*—jugal fold, M—Media, m—medial cell, *mnfl*—median flexion line, psp—posterior spiracle, R1—first branch of radius, r1—first radial cell, R2+3—fused second and third branch of radius, r2+3—second and third radial cell, R4+5—fused fourth and fifth branch of radius, r4+5—fourth and fifth radial cell, r-m—radio-medial cross vein, rp—resilin patch, Sc—subcosta, sc—subcostal cell, Scb—subcostal break, sc—scutum, scl—scutellum, *sfl*—squamal flexion line, *tfl1*—transverse flexion line 1, *tfl2*—transverse flexion line 2, tr—trachea, ts—thoracic squama, vf1, 2—first and second dorsal field of haltere campaniform sensilla, vg1-3——first, second and third group of campaniform sensilla on the ventral side of the wing, versus—single campaniform sensilla on the ventral wing side (nomenclature adapted from.[234,235] Scale bars: B,H) 50 µm, C,F,G) 100 µm, D) 10 µm, E) 500 µm.

flexible resilin-containing structures have an overall effect on the entire wing, influencing, e.g., the mitigation of collision damage or large-scale wing deformations like camber and, thereby, its aerodynamic performance. As insect wings lack internal muscles, resilin additionally supports (asymmetric) directional passive wing deformations, e.g., along precisely defined fold lines, which allow, e.g., earwigs to fold their wings even passively without any muscular force. All these functions are critical for the insect's survival, and due to its long fatigue life, resilin ensures the structures' functionability for millions and millions of cycles.

Interestingly, in nature (unlike most of the synthetically produced RLPs), resilin only rarely occurs in its pure form but is usually mixed with chitin fibers that alter the material properties of the respective structures according to their arrangement and thereby enable a direction-dependent behavior. Whereas some overall strongly sclerotized structures are embedded in a flexible, resilin-bearing base, resilin-containing structures often do not abruptly transition to strongly sclerotized cuticle but show a rather smooth gradient, thereby improving the systems performance. Others are additionally combined with structurally extensible structures like microfolds.

Apart from influencing the elastic behavior of resilin in terms of its mixture with chitin fibers and its arrangement in the supporting structure, studies on the sequence of natural resilin and resilin-like polypeptides have revealed various factors (as, e.g., the proportion of hydrophilic to hydrophobic amino acids, the amount of dityrosine crosslinks, the amounts of proline, glycine and alanine, the number and length of elastic repeat motifs, etc.), which allow an adaptation of the protein's structure, stiffness, stimuli-responsiveness to, e.g., pH, temperature or mechanical stress and its capability to self-assemble. Including secondary domains of other proteins in the form of modular RLPs even widens the potential fields of applications for resilin-like polypeptides in various medical and industrial applications. However, although significant progress has been made in understanding the structure-function relationship of disordered proteins like resilin and many putative resilin-like proteins have been identified in various insect species via sequence analyses as well as microscopical and mechanical testing, we still can only hypothesize about the potential resilience, environmental factors like the hydration level throughout the insect's life, the behavior and extent of deformation during, e.g., the wing beat cycle and the complex function of chitin-resilin(-like proteins) composites in natural systems, and even questions like how the rare dual-phase transition behavior (with upper and lower critical solution temperature) is encoded in the RLP structure and sequence or how much glycine and proline resilin needs to be structurally disordered or responsive to multiple stimuli remain elusive so far.[9,10,19]

Acknowledgements

The authors thank Karolyn Darrow and Sean Brady of the Smithsonian National Museum of Natural History (Department of Entomology, United States) for kindly providing photographs of the wings of *Poecilopompilus algidus*.

Open access funding enabled and organized by Projekt DEAL.

Conflict of Interest

The authors declare no conflict of interest.

Author Contributions

E.A.: conceptualization; investigation; writing—original draft, review & editing; J.M.: conceptualization; investigation; writing—review & editing; S. N.G.: conceptualization; writing— review & editing.

Keywords

energy storage, insect flight, resilin, wing deformation

Received: December 29, 2022
Revised: June 1, 2023
Published online: August 18, 2023

[1] S. O. Andersen, in *Elastomeric Proteins: Structures, Biomechanical Properties, and Biological Roles* (Eds: P. Shewry, A. Tatham, A. Bailey), Cambridge University Press, Cambridge **2003**, Ch. 13.
[2] S. Rauscher, R. Pomès, in *Fuzziness: Structural Disorder in Protein Complexes*, Advances in Experimental Medicine and Biology, Vol. *725*, (Eds: M. Fuxreiter, P. Tompa), Springer, New York **2012**, Ch. 10.
[3] S. O. Andersen, T. Weis-Fogh T, *Adv. Insect Physiol.* **1964**, *2*, 1.
[4] T. Weis-Fogh, *J. Exp. Biol.* **1960**, *37*, 889.
[5] M. Jensen, T. Weis-Fogh, *Philos. Trans. R. Soc., B* **1962**, *245*, 137.
[6] J. Gosline, M. Lillie, E. Carrington, P. Guerette, C. Ortlepp, K. Savage, *Philos. Trans. R. Soc., B* **2002**, *357*, 121.
[7] C. M. Elvin, A. G. Carr, M. G. Huson, J. M. Maxwell, R. D. Pearson, T. Vuocolo, N. E. Liyou, D. C. C. Wong, D. J. Merritt, N. E. Dixon, *Nature* **2005**, *437*, 999.
[8] R. E. Lyons, D. C. Wong, M. Kim, N. Lekieffre, M. G. Huson, T. Vuocolo, D. J. Merritt, K. M. Nairn, D. M. Dudek, M. L. Colgrave, C. M. Elvin, *Insect Biochem. Mol. Biol.* **2011**, *41*, 881.
[9] R. Balu, N. K. Dutta, A. K. Dutta, N. R. Choudhury, *Nat. Commun.* **2021**, *12*, 149.
[10] S. S. Patkar, C. G. Garcia, K. L. Kiick, in *Biomimetic Protein Based Elastomers - Emerging Materials for the Future* (Eds: N. R. Choudhury, J. C. Liu, N. K. Dutta), Royal Society of Chemistry, London **2022**, pp. 73–99, Ch. 4.
[11] M. B. Charati, J. L. Ifkovits, J. A. Burdick, J. G. Linhardt, K. L. Kiick, *Soft Matter* **2009**, *5*, 3412.
[12] R. S.-C. Su, R. J. Jr Galas, C.-Y. Lin, J. C. Liu, *Macromol. Biosci.* **2019**, *19*, 1900122.
[13] I. Weitzhandler, M. Dzuricky, I. Hoffmann, F. G. Quiroz, M. Gradzielski, A. Chilkoti, *Biomacromolecules* **2017**, *18*, 2419.
[14] W. Fang, M. V. Nonappa, P. Mohammadi, S. Koskela, M. Soikkeli, A. Westerholm-Parvinen, C. P. Landowski, M. Penttilä, M. B. Linder, P. Laaksonen, *Colloids Surf., B* **2018**, *171*, 590.
[15] A. Griffo, H. Hähl, S. Grandthyll, F. Müller, A. Paananen, M. Ilmén, G. R. Szilvay, C. P. Landowski, M. Penttilä, K. Jacobs, P. Laaksonen, *ACS Omega* **2017**, *2*, 6906.
[16] R. Balu, R. Knott, C. M. Elvin, A. J. Hill, N. R. Choudhury, N. K. Dutta, *Biosensors* **2019**, *9*, 128.
[17] R. E. Lyons, C. M. Elvin, K. Taylor, N. Lekieffre, J. A. M. Ramshaw, *Biotechnol. Bioeng.* **2012**, *109*, 2947.
[18] M. S. Khandaker, D. M. Dudek, E. P. Beers, D. A. Dillard, D. R. Bervan, *J. Mech. Behav. Biomed. Mater.* **2016**, *61*, 110.
[19] S. O. Andersen, *Insect Biochem. Mol. Biol.* **2010**, *40*, 541.
[20] D. H. Ardell, S. O. Andersen, *Insect Biochem. Mol. Biol.* **2001**, *31*, 965.
[21] G. Qin, S. Lapidot, K. Numata, X. Hu, S. Meirovitch, M. Dekel, I. Podoler, O. Shoseyov, D. L. Kaplan, *Biomacromolecules* **2009**, *10*, 3227.

[22] R. S.-C. Su, Y. Kim, J. C. Liu, *Acta Biomater.* **2014**, *10*, 1601.
[23] G. Qin, A. Rivkin, S. Lapidot, X. Hu, I. Preis, S. B. Arinus, O. Dgany, O. Shoseyov, D. L. Kaplan, *Biomaterials* **2011**, *32*, 9231.
[24] G. Qin, X. Hu, P. Cebe, D. L. Kaplan, *Nat. Commun.* **2012**, *3*, 1003.
[25] *Rubberlike Elasticity: A Molecular Primer* (Eds: J. E. Mark, B. Erman), Cambridge University Press, Cambridge **2007**.
[26] T. Weis-Fogh, *Nature* **1970**, *227*, 718.
[27] S. O. Andersen, *Insect Biochem. Mol. Biol.* **2004**, *34*, 459.
[28] S. O. Andersen, *Acta Physiol. Scand.* **1966**, *263*, 1.
[29] A. C. Neville, *J. Insect Physiol.* **1963**, *9*, 177.
[30] A. C. Neville, *J. Cell Sci.* **1967**, *2*, 273.
[31] A. M. Tamburro, S. Panariello, V. Santopietro, A. Bracalello, B. Bochicchio, A. Pepe, *ChemBioChem* **2010**, *11*, 83.
[32] J. H. Willis, *Insect Biochem. Mol. Biol.* **2010**, *40*, 189.
[33] S. O. Andersen, *Ann. Rev. Entomol.* **1979**, *24*, 29.
[34] S. Rauscher, S. Baud, M. Miao, F. W. Keeley, R. Pomès, *Structure* **2006**, *14*, 1667.
[35] S. Cheng, M. Cetinkaya, F. Gräter, *Biophys. J.* **2010**, *99*, 3863.
[36] A. A. Adzhubei, M. J. Sternberg, A. A. Makarov, *J. Mol. Biol.* **2013**, *425*, 2100.
[37] K. N. Savage, J. M. Gosline, *J. Exp. Biol.* **2008**, *211*, 1937.
[38] K. N. Savage, J. M. Gosline, *J. Exp. Biol.* **2008**, *211*, 1948.
[39] K. Bailey, T. Weis-Fogh, *Biochim. Biophys. Acta* **1961**, *48*, 452.
[40] R. Balu, R. Knott, N. P. Cowieson, C. M. Elvin, A. J. Hill, N. R. Choudhury, N. K. Dutta, *Sci. Rep.* **2015**, *5*,10896.
[41] L. Li, S. Teller, R. J. Clifton, X. Jia, K. L. Kiick, *Biomacromolecules* **2011**, *12*, 2302.
[42] L. Li, Z. Tong, X. Jia, K. L. Kiick, *Soft Matter* **2013**, *9*, 665.
[43] M. Y. Truong, N. K. Dutta, N. R. Choudhury, M. Kim, C. M. Elvin, K. M. Nairn, A. J. Hill, *Biomaterials* **2011**, *32*, 8462.
[44] R. Balu, J. Whittaker, N. K. Dutta, C. M. Elvin, N. R. Choudhury, *J. Mater. Chem. B* **2014**, *2*, 5936.
[45] A. Kovalev, A. Filippov, S. N. Gorb, *J. Comp. Physiol., A* **2018**, *204*, 409.
[46] S. Lerch, R. Zuber, N. Gehring, Y. Wang, B. Eckel, K.-D. Klass, F.-O. Lehmann, B. Moussian, *BMC Biol.* **2020**, *18*, 195.
[47] H. Peisker, J. Michels, S. N. Gorb, *Nat. Commun.* **2013**, *4*, 1661.
[48] A. C. Neville, *J. Insect Physiol.* **1963**, *9*, 265.
[49] S. O. Andersen, *Biochim. Biophys. Acta* **1963**, *69*, 249.
[50] S. O. Andersen, *J. Exp. Biol.* **1966**, *44*, 119.
[51] J. Michels, S. N. Gorb, *J. Microsc.* **2012**, *245*, 1.
[52] J. Michels, E. Appel, S. N. Gorb, *Extracellular Composite Matrices in Arthropods*, Springer International Publishing, Cham, Switzerland **2016**.
[53] J. Michels, E. Appel, S. N. Gorb, *Beilstein J. Nanotechnol.* **2016**, *7*, 1241.
[54] H. C. Bennet-Clark, E. C. A. Lucey, *J. Exp. Biol.* **1967**, *47*, 59.
[55] D. Young, H. C. Bennet-Clark, *J. Exp. Biol.* **1995**, *198*, 1001.
[56] S. N. Gorb, *Arthropod Struct. Dev.* **2004**, *33*, 201.
[57] P. P. Goodwyn, A. Peressadko, H. Schwarz, V. Kastner, S. N. Gorb, *J. Comp. Physiol., A* **2006**, *192*, 1233.
[58] L. Koerner, S. N. Gorb, O. Betz, *Zoology* **2012**, *115*, 117.
[59] J. Michels, J. Vogt, S. N. Gorb, *Sci. Rep.* **2012**, *2*, 465.
[60] J. Michels, S. N. Gorb, K. J. Reinhardt, *J. R. Soc., Interface* **2015**, *12*, 20141107.
[61] S. N. Gorb, *Naturwissenschaften* **1999**, *86*, 552.
[62] F. Haas, S. N. Gorb, R. J. Wootton, *Arthropod Struct. Dev.* **2000**, *29*, 137.
[63] F. Haas, S. N. Gorb, R. Blickhan, *Proc. Biol. Sci.* **2000**, *267*, 1375.
[64] M. Burrows, *J. Exp. Biol.* **2010**, *213*, 469.
[65] E. Appel, L. Heepe, C. P. Lin, S. N. Gorb, *J Anat.* **2015**, *227*, 561.
[66] E. Appel, J. Michels, S. N. Gorb, in *Biomimetic Protein Based Elastomers: Emerging Materials for the Future* (Eds: N. R. Choudhurry, J. C. Liu, N. B. Dutta), Royal Society of Chemistry, London **2022**, Ch. 2.
[67] D. Grimaldi, M. S. Engel, in *Evolution of the Insects*, Cambridge University Press, Cambridge **2005**.
[68] B. Misof, S. Liu, K. Meusemann, R. S. Peters, A. Donath, C. Mayer, P. B. Frandsen, J. Ware, T. Flouri, R. G. Beutel, O. Niehuis, M. Petersen, F. Izquierdo-Carrasco, T. Wappler, J. Rust, A. J. Aberer, U. Aspöck, H. Aspöck, D. Bartel, A. Blanke, S. Berger, A. Böhm, T. R. Buckley, B. Calcott, J. Chen, F. Friedrich, M. Fukui, M. Fujita, C. Greve, P. Grobe, *Science* **2014**, *346*, 763.
[69] D. E. Alexander, *Arthropod Struct. Dev.* **2018**, *47*, 322.
[70] R. Moreau, L. Lavenseau, *J. Insect Physiol.* **1975**, *21*, 1531.
[71] L. T. Wasserthal, *Experientia* **1976**, *32*, 577.
[72] C. J. H. Elliott, *J. Insect Physiol.* **1981**, *27*, 695.
[73] J. A. Kiger, J. E. Natzle, M. M. Green, *Proc. Natl. Acad. Sci. USA* **2001**, *98*, 10190.
[74] K. Kimura, A. Kodama, Y. Hayasaka, Y. T. Ohta, *Development* **2004**, *131*, 1597.
[75] M. Tögel, G. Pass, A. Paululat, *Dev. Biol.* **2008**, *318*, 29.
[76] S. Aldaz, L. M. Escudero, M. Freeman, *Proc. Natl. Acad. Sci. USA* **2010**, *107*, 14217.
[77] J. V. Beira, R. Paro, *Chromosoma* **2016**, *125*, 573.
[78] N. A. Dye, M. Popović, S. Spannl, R. Etournay, D. Kainmüller, S. Ghosh, E. W. Myers, F. Jülicher, S. Eaton, *Development* **2017**, *144*, 4406.
[79] G. Pass, *Arthopod Struct. Dev.* **2018**, *47*, 391.
[80] M. K. Salcedo, J. Socha, *Integr. Comp. Biol.* **2020**, *60*, 1208.
[81] J. W. Arnold, *Mem. Entomol. Soc. Can.* **1964**, *38*, 5e60.
[82] J. F. Hillyer, G. Pass, *Ann. Rev. Entomol.* **2020**, *65*, 121.
[83] H. W. Krenn, G. Pass, *Zoology* **1994**, *98*, 7e22.
[84] H. W. Krenn, G. Pass, *Zoology* **1995**, *98*, 147.
[85] M. K. Salcedo, B. Jun, P. Vlachos, L. Mahadevan, S. A. Combes, *bioRxiv* **2021**, 2021.09.15.460448.
[86] R. Guillermo-Ferreira, E. Appel, P. Urban, P. C. Bispo, S. N. Gorb, *Biol. Lett.* **2017**, *13*, 20160960.
[87] J. F. V. Vincent, U. G. K. Wegst, *Arthropod Struct. Dev.* **2004**, *33*, 189.
[88] S. Enders, N. Barbakadse, S. N. Gorb, E. Arzt, *J. Mater. Res.* **2004**, *19*, 880.
[89] A. M. Mountcastle, T. L. Daniel, *Exp. Fluids* **2009**, *45*, 873.
[90] T. Mengesha, R. Vallance, R. Mittal, *Bioinspiration Biomimetics* **2010**, *6*, 014001.
[91] D. Klocke, H. Schmitz, *Acta Biomater.* **2011**, *7*, 2935.
[92] J.-H. Dirks, D. Taylor, *PLoS One* **2012**, *7*, e43411.
[93] Y. H. Chen, S. Martin, Y. Zhao, W. M. Huang, *Mater. Lett.* **2013**, *97*, 166.
[94] S. Clare, O. E. Tauber, *Ann. Entomol. Soc. Am.* **1942**, *35*, 57.
[95] J. W. Arnold, *Ann. Entomol. Soc. Am.* **1959**, *52*, 229.
[96] L. T. Wasserthal, *Zoomorphology* **1983**, *103*, 177.
[97] H. Rajabi, V. Schroeter, S. Eshghi, S. N. Gorb, *Biol. Open* **2017**, *6*, 1290.
[98] H. Rajabi, J.-H. Dirks, S. N. Gorb, *J. Exp. Biol.* **2020**, *223*, jeb215194.
[99] J. Rudolf, L.-Y. Wang, S. N. Gorb, H. Rajabi, *Biomed. Mater.* **2019**, *99*, 127.
[100] D. Hou, Y. Yin, H. Zhao, Z. Zhong, *Comput. Biol. Med.* **2015**, *58*, 14.
[101] D. Hou, Y. Yin, Z. Zhong, H. Zhao, *Bioinspiration Biomimetics* **2015**, *10*, 016020.
[102] R. K. Norberg, *J. Comp. Physiol.* **1972**, *81*, 9.
[103] J. Fabian, I. Siwanowicz, M. Uhrhan, M. Meada, R. J. Bomphrey, H.-T. Lin, *bioRxiv* **2021**, 2021.04.11.439336.
[104] H. C. Bennet-Clark, *Sci. Prog.* **1975**, *62*, 263.
[105] H. López, M. D. García, E. Clemente, J. J. Presa, P. Oromí, *J. Zool.* **2008**, *275*, 1.
[106] C. Luo, C. Wei, *PLoS One* **2015**, *10*, e0118667.

[107] T. B. H. Schroeder, J. Houghtaling, B. D. Wilts, M. Mayer, *Adv. Mater.* **2018**, *30*, 1705322.
[108] L. T. Wasserthal, *J. Insect Physiol.* **1975**, *21*, 1921.
[109] L. P. Biró, Zs. Bálint, K. Kertész, Z. Vértesy, G. I. Márk, Z. E. Horváth, J. Balázs, D. Méhn, I. Kiricsi, V. Lousse, J.-P. Vigneron, *Phys. Rev. E: Stat., Nonlinear, Soft Matter Phys.* **2003**, *67*, 021907.
[110] Y. Obara, T. Hidaka, *Proc. Jpn. Acad.* **1968**, *44*, 829.
[111] D. Hilfert-Rüppell, G. Rüppell, *Int. J. Odonatol.* **2013**, *16*, 119.
[112] R. Guillermo-Ferreira, P. C. Bispo, E. Appel, A. Kovalev, S. N. Gorb, *J. Insect Physiol.* **2015**, *81*, 129.
[113] Y. Tomoyasu, Y. Arakane, K. J. Kramer, R. E. Denell, *Curr. Biol.* **2009**, *19*, 2057.
[114] D. M. Linz, A. W. Hu, M. I. Sitvarin, Y. Tomoyasu, *Sci. Rep.* **2016**, *6*, 34813.
[115] R. J. Wootton, *Annu. Rev. Entomol.* **1992**, *37*, 113.
[116] R. J. Wootton, *Insects* **2020**, *11*, 446.
[117] R. J. Wootton, *J. Zool.* **1981**, *193*, 447.
[118] D. J. S. Newman, R. J. Wootton, *J. Exp. Biol.* **1986**, *125*, 361.
[119] A. M. Mountcastle, S. A. Combes, *J. Exp. Biol.* **2014**, *217*, 1108.
[120] R. Ennos, *J. Exp. Biol.* **1989**, *142*, 87.
[121] S. R. Jongerius, D. Lentink, *Exp. Mech.* **2010**, *50*, 1323.
[122] R. J. Wootton, *Zool. Scr.* **2002**, *31*, 31.
[123] R. J. Wootton, R. C. Herbert, P. G. Young, K. E. Evans, *Philos. Trans. R. Soc., B* **2003**, *358*, 1577.
[124] A. R. Ennos, *Proc. R. Soc. London, Ser. B* **1995**, *259*, 15.
[125] C. P. Ellington, C. Van Den Berg, A. P. Willmott, A. L. R. Thomas, *Nature* **1996**, *384*, 626.
[126] R. J. Wootton, *J. Exp. Biol.* **1993**, *180*, 105.
[127] T. Engels, H.-N. Wehmann, F.-O. Lehmann, *J. R. Soc.,Interface* **2020**, *17*, 20190804.
[128] M. Okamoto, K. Yasuda, A. Azuma, *J. Exp. Biol.* **1996**, *199*, 281.
[129] R. R. Harbig, J. Sheridan, M. C. Thompson, *J. Fluid Mech.* **2013**, *730*, 52.
[130] T. Q. Le, T. V. Truong, H. T. Tran, S. H. Park, J. H. Ko, H. C. Park, K. J. Yoon, D. Byun, *J. Bionic Eng.* **2013**, *10*, 316.
[131] J. Feaster, F. Battaglia, J. A. Bayandor, *Biol. Open* **2017**, *6*, 1784.
[132] C. J. C. Rees, *Nature* **1975**, *258*, 141.
[133] A. B. Kesel, *J. Exp. Biol.* **2000**, *203*, 3125.
[134] W.-K. Kim, J. H. Ko, H. C. Park, D. Byun, *J. Theor. Biol.* **2009**, *260*, 523.
[135] D.-E. Levy, A. Seifert, *Phys. Fluids* **2009**, *21*, 071901.
[136] G. Du, M. Sun, *J. Theor. Biol.* **2012**, *300*, 19.
[137] K. Hord, Y. Liang, *J. Aircr.* **2012**, *49*, 749.
[138] C. J. Barnes, M. R. Visbal, *Phys. Fluids* **2013**, *25*, 115106.
[139] X. G. Meng, S. Mao, *Phys. Fluids* **2013**, *25*, 071905.
[140] Y. Chen, M. Skote, *J. Fluid Struct.* **2016**, *62*, 1.
[141] A. Shahzad, H. R. Hamdani, A. Aizaz, *J. Appl. Fluid Dyn.* **2017**, *10*, 833.
[142] M. I. Ansari, S. F. Anwer, *Fluid Dyn. Mater. Process.* **2018**, *14*, 259.
[143] S. Krishna, M. Cho, H.-N. Wehmann, T. Engels, F.-O. Lehmann, *Insects* **2020**, *11*, 466.
[144] T. Weis-Fogh, *J. Mol. Biol.* **1961**, *3*, 648.
[145] A. C. Neville, *J. Exp. Biol.* **1960**, *37*, 631.
[146] R. J. King, *Master's Thesis, Virginia Polytechnic Institute and State University*, **2010**.
[147] F. Bäumler, S. Büsse, *Biol. Lett.* **2019**, *15*, 20190127.
[148] D. P. A. Neff, *Doctoral Thesis*, Marshall University, West Virginia **2012**.
[149] T. Weis-Fogh, *J. Exp. Biol.* **1973**, *59*, 169.
[150] R. E. Snodgrass, *Smithson. Misc. Collect.* **1929**, *82*, 1.
[151] W. Nachtigall, A. Wisser, D. Eisinger, *J. Comp. Physiol., B* **1998**, *168*, 323.
[152] U. Choudhury, *Master's Thesis*, Virginia Polytechnic Institute and State University, **2012**.
[153] B. Jäckle, *Diploma thesis*, Eberhard Karls University of Tübingen, **2003**.
[154] E. Appel, S. N. Gorb, *Bioinspiration Biomimetics* **2011**, *6*, 046006.
[155] E. Appel, S. N. Gorb, in *Zoologica*, (Ed: H. F. Paulus), Schweizerbart Science Publishers, Stuttgart, Germany **2014**, pp. 1–104.
[156] S. Donoughe, J. D. Crall, R. A. Merz, S. A. Combes, *J. Morphol.* **2011**, *272*, 1409.
[157] A. G. Richards, A. Richards, *Int. J. Insect Morphol. Embryol.* **1979**, *8*, 143.
[158] D. J. S. Newman, *Ph.D. thesis*, University of Exeter, **1982**.
[159] G. Bechly, *Petalura* **1996**, *2*, 1.
[160] H. Rajabi, N. Ghoroubi, A. Darvizeh, J.-H. Dirks, E. Appel, S. N. Gorb, *Bioinspiration Biomimetics.* **2015**, *10*, 056003.
[161] H. Rajabi, A. Shafiei, A. Darvizeh, S. N. Gorb, *Sci. Rep.* **2016**, *6*, 39039.
[162] M. Noorhidayah, K. Yazawa, K. Numata, Y. Norma-Rashid, *PLoS One* **2018**, *13*, e0193147.
[163] H. Rajabi, A. Shafiei, A. Darvizeh, J.-H. Dirks, E. Appel, S. N. Gorb, *R. Soc. Open Sci.* **2016**, *3*, 150610.
[164] H. Rajabi, N. Ghoroubi, K. Stamm, E. Appel, S. N. Gorb, *Acta Biomater.* **2017**, *60*, 330.
[165] A. R. Ennos, *J. Exp. Biol.* **1988**, *140*, 137.
[166] H. Rajabi, A. Shafiei, A. Darvizeh, J.-H. Dirks, E. Appel, S. N. Gorb, *R. Soc. Open Sci.* **2016**, *3*, 160006.
[167] B. N. Danforth, *J. Zool.* **1989**, *218*, 247.
[168] B. N. Danforth, C. D. Michener, *Ann. Entomol. Soc. Am.* **1988**, *81*, 342.
[169] I. Mikó, R. S. Copeland, J. P. Balhoff, M. J. Yoder, A. R. Deans, *PLoS One* **2014**, *9*, e94056.
[170] R. F. Chapman, in *The Insects: Structure and Function*, 5th ed., (Eds: S. J. Simpson, A. E. Douglas), Cambridge University Press, Cambridge, **2013**, pp. 193–230.
[171] R. J. Wootton, *Syst. Entomol.* **1979**, *4*, 81.
[172] J. H. Brackenbury, *J. Zool.* **1994**, *233*, 523.
[173] W. R. M. Mason, *Proc. Entomol. Soc. Wash.* **1986**, *88*, 1.
[174] R. Dudley, in *The Biomechanics of Insect Flight: Form, Function, Evolution*, Princeton University Press, Princeton, New Jersey **2000**, pp. 36–74.
[175] O. W. Richards, in *RES Handbooks for the Identification of British Insects*, Vol. *6*, 2nd ed., (Ed: A. Watson), Royal Entomological Society of London, St Albans, UK **1977**.
[176] Y. Ma, T. Ma, J. Ning, S. N. Gorb, *Soft Matter* **2020**, *16*, 4057.
[177] A. M. Mountcastle, S. A. Combes, *Proc. R. Soc. B* **2013**, *280*, 20130531.
[178] Y. Ma, J. G. Ning, H. L. Ren, P. F. Zhang, H. Y. Zhao, *J. Exp. Biol.* **2015**, *218*, 2136.
[179] B. L. Fisher, B. Bolton, *Ants of Africa and Madagaskar: A Guide to the Genera*, University of California Press, Oakland, CA **2016**.
[180] G. F. Edmunds, J. R. Traver, *J. Wash. Acad. Sci.* **1954**, *44*, 390.
[181] E. Dominguez, V. Abdala, *J. Morphol.* **2019**, *280*, 95.
[182] R. J. Bomphrey, G. K. Taylor, A. L. R. Thomas, *Exp. Fluids* **2009**, *46*, 811.
[183] J. G. Ning, Y. Ma, H. L. Ren, P. F. Zhang, *Biol. Open* **2017**, *6*, 619.
[184] J. T. Vance, S. P. Roberts, *J. Insect Physiol.* **2014**, *65*, 27.
[185] J. C. Roberts, R. V. Catar, *Can. J. Zool.* **2015**, *93*, 531.
[186] J. Zhao, M. Xu, Y. Liang, S. Yan, W. Niu, *J. Insect Physiol.* **2018**, *109*, 100.
[187] J. Kukalová-Peck, *Psyche* **1974**, *81*, 315.
[188] J. Kukalová-Peck, *Psyche* **1974**, *81*, 416.
[189] J. Kukalová-Peck, *J. Morphol.* **1978**, *156*, 53.
[190] J. Willkommen, *Stuttg. Beitr. Naturk. D. Ser. A (Biol.)* **2008**, *1*, 203.
[191] F. Haas, *Arthropod Syst. Phylog.* **2006**, *64*, 149.
[192] U. N. Lanham, *J. N. Y. Entomol. Soc.* **1977**, *85*, 98.

[193] H. H. Basibuyuk, D. L. J. Quicke, *J. Bombay Nat. Hist. Soc.* **1997**, *31*, 1563.
[194] Y. Ma, H. Ren, J. Ning, S. N. Gorb, *Soft Matter* **2022**, *18*, 956.
[195] I. Stocks, doctoral thesis, Clemson University, South Carolina **2009**.
[196] J. Michels, E. Appel, S. N. Gorb, *Arthropod Struct. Dev.* **2021**, *60*, 101008.
[197] Y. Ma, H. Ren, H. Rajabi, H. Zhao, J. Ning, S. N. Gorb, *J. Insect Physiol.* **2019**, *118*, 103936.
[198] A. Toofani, S. H. Eraghi, M. Khorsandi, A. Khaheshi, A. Darvizeh, S. N. Gorb, H. Rajabi, *Acta Biomater.* **2020**, *110*, 188.
[199] H. F. Schwarz, *Bull. Am. Mus. Nat. Hist.* **1948**, *90*, 1.
[200] D. P. Abrol, *J. Anim. Morphol. Physiol.* **1986**, *3*, 107.
[201] F. Haas, *PhD Thesis*, University of Jena, **1998**.
[202] P. M. Hammond, in *Carabid Beetles* (Eds: T. L. Erwin, G. E. Ball, D. R. Whitehead, A. L. Halpern), Springer, Dordrecht, Netherlands **1979**, pp. 113–180.
[203] F. Haas, R. G. Beutel, *Zoology* **2001**, *104*, 123.
[204] D. N. Fedorenko, *Biol. Bull. Rev.* **2015**, *5*, 71.
[205] F. Haas, R. J. Wootton, *Proc. R. Soc. London, Ser. B* **1996**, *263*, 1651.
[206] J. H. Brackenbury, in *IUTAM-IASS Symposium on Deployable Structures: Theory and Applications. Solid Mechanics and Its Applications*, Vol. *80* (Eds: S. Pellegrino, S. D. Guest), Springer, Dordrecht, the Netherlands **2000**, pp. 37–44.
[207] T. Geisler, *Acta Mech. Autom.* **2012**, *6*, 37.
[208] N. S. Ha, Q. T. Truong, N. S. Goo, H. C. Park, *PLoS One* **2013**, *8*, e80689.
[209] K. Saito, S. Yamamoto, M. Maruyama, Y. Okabe, *Proc. Natl. Acad. Sci. USA* **2014**, *111*, 16349.
[210] Z. Linghu, C. Zhao, H. Yang, X. Zheng, *Sci. Bull.* **2015**, *60*, 1457.
[211] K. Saito, S. Nomura, S. Yamamoto, R. Niyama, Y. Okabe, *Proc. Natl. Acad. Sci. USA* **2017**, *114*, 5624.
[212] Z. Song, Y. Yan, J. Tong, J. Sun, *J. Mater. Sci.* **2020**, *55*, 4524.
[213] H. V. Phan, H. C. Park, *Science* **2020**, *370*, 1214.
[214] Z. Song, J. Tong, W. Pfleging, J. Sun, *Comput. Biol. Med.* **2021**, *133*, 104397.
[215] Z. Song, J. Tong, Y. Yan, W. W. Wu, L. Tian, J. Sun, *Micron* **2020**, *140*, 102965.
[216] X. Li, C. Guo, L. Li, *Anim. Cells Syst.* **2019**, *23*, 143.
[217] Y. Meresman, G. Ribak, *J. Exp. Biol.* **2020**, *233*, jeb225599.
[218] W. Kleinow, *Z. Morphol. Oekol. Tiere* **1966**, *56*, 363.
[219] J. Deiters, W. Kowalczyk, T. Seidl, *Biol. Open* **2016**, *5*, 638.
[220] F. Haas, J. Kukalová-Peck, *Eur. J. Entomol.* **2001**, *98*, 445.
[221] F. Haas, J. T. C. Hwen, H. B. Tang, *Arthropod. Syst. Phylog.* **2012**, *70*, 95.
[222] F. Haas, *Acta Zool. Cracov.* **2003**, *46*, 67.
[223] J. Deiters, W. Kowalczyk, T. Seidl, in *Bionik: Patente aus der Natur - Tagungsbeiträge zum 7. Bionik-Kongress* (Eds: A. B. Kesel, D. Zehren), Bionik- Innovations-Centrum (B-I-C), Bremen **2015**, pp. 187–191.
[224] J. A. Faber, A. F. Arrieta, A. R. Studart, *Science* **2018**, *359*, 1386.
[225] M. A. Frye, J. R. Gray, in *Methods in Insect Sensory Neuroscience* (Ed: T. A. Christensen), CRC Press, Boca Raton, Florida **2005**, pp. 107.
[226] A. M. Yarger, J. L. Fox, *Integr. Comp. Biol.* **2016**, *56*, 865.
[227] F.-O. Lehmann, J. Bartussek, *J. Comp. Physiol., A* **2017**, *203*, 1.
[228] J. M. Hall, D. P. McLoughlin, N. D. Kathman, A. M. Yarger, S. Mureli, J. L. Fox, *Biol. Lett.* **2015**, *11*, 20150845.
[229] W. Pix, G. Nalbach, J. Zeil, *Naturwissenschaften* **1993**, *80*, 371.
[230] S. P. Sane, A. Dieudonné, M. A. Willis, T. L. Daniel, *Science* **2007**, *315*, 863.
[231] B. H. Dickerson, Z. N. Aldworth, T. L. Daniel, *J. Exp. Biol.* **2014**, *217*, 2301.
[232] R. F. Chapman, *The Insects: Structure and Function*, 4th ed., Cambridge University Press, Cambridge **1998**.
[233] S. M. Walker, A. L. Thomas, G. K. Taylor, *J. R. Soc., Interface* **2012**, *9*, 1194.
[234] W. Gnatzy, U. Grünert, M. Bender, *Zoomorphology* **1987**, *106*, 312.
[235] J. F. McAlpine, in *Nearctic Diptera*, Vol. *1*, (Eds: J. F. McAlpine, B. V. Peterson, G. E. Shewell, H. J. Teskey, J. R. Vockeroth, D. M. Wood), Agriculture Canada, Ottawa **1981**, pp. 2–56.
[236] F.-O. Lehmann, S. N. Gorb, N. Nasir, P. Schützner, *J. Exp. Biol.* **2011**, *214*, 2949.
[237] H. Wehmann, L. Heepe, S. N. Gorb, T. Engels, F.-O. Lehmann, *Biol. Open* **2019**, *8*, bio038299.
[238] A. R. Ennos, *J. Linn. Soc. London, Zool.* **1989**, *96*, 27.
[239] A. B. Kesel, U. Philippi, W. Nachtigall, *Comput. Biol. Med.* **1998**, *28*, 423.
[240] R. L. Chevalier, *J. Morphol.* **1969**, *128*, 443.
[241] E. S. Cole, J. Palka, *J. Embryol. Exp. Morphol.* **1982**, *71*, 41.
[242] M. H. Dickinson, J. Palka, *J. Neurosci.* **1987**, *7*, 4201.
[243] U. Grünert, W. Gnatzy, *Zoomorphology* **1987**, *106*, 320.
[244] J. W. S. Pringle, *Philos. Trans. R. Soc., B* **1948**, *602*, 347.
[245] D. T. Moran, K. M. Chapman, R. A. Ellis, *J. Cell Biol.* **1971**, *48*, 155.
[246] A. Fayyazuddin, M. H. Dickinson, *J. Neurosci.* **1996**, *16*, 5225.
[247] W. D. Wiesenborn, *Psyche* **2011**, *2011*, 875250.
[248] W. P. Chan, F. Prete, M. H. Dickinson, *Science* **1998**, *280*, 289.
[249] R. Parween, R. Pratap, *Biol. Open* **2015**, *4*, 137.
[250] T. Deora, A. K. Singh, S. P. Sane, *Proc. Natl. Acad. Sci. USA* **2015**, *112*, 1481.
[251] G. Nalbach, *J. Comp. Physiol., A* **1993**, *173*, 293.
[252] A. L. Eberle, B. H. Dickerson, P. G. Reinhall, T. L. Daniel, *J. R. Soc., Interface* **2015**, *12*, 20141088.
[253] M. H. Dickinson, *J. Exp. Biol.* **1990**, *151*, 245.
[254] M. H. Dickinson, *J. Exp. Biol.* **1992**, *169*, 221.
[255] W. P. Chan, M. H. Dickinson, *J. Comp. Neurol.* **1996**, *369*, 405.
[256] N. D. Kathman, J. L. Fox, *J. Neurosci.* **2019**, *39*, 4100.

Esther Appel received her diploma in biology from Kiel University in 2011. She is currently working with Prof. Stanislav Gorb at the Institute of Zoology at Kiel University. Her research focuses on the functional morphology of insect wings with an emphasis on dragonflies and damselflies.

Jan Michels studied biological oceanography, zoology, and marine chemistry at Kiel University. He then investigated the role of copepods in cryo-pelago-benthic coupling in the Southern Ocean at the Alfred Wegener Institute Helmholtz Centre for Polar and Marine Research in Bremerhaven and received his Ph.D. in biological oceanography from Kiel University. Subsequently, he was a postdoctoral fellow in the Department of Functional Morphology and Biomechanics at Kiel University and in the GEOMAR Helmholtz Centre for Ocean Research Kiel. His scientific interests strongly focus on the application of microscopy techniques and methods to investigate the morphology and composition of arthropod exoskeleton structures.

Stanislav N. Gorb is Professor and Director at the Zoological Institute of the Kiel University, Germany. He received his PhD degree in zoology and entomology at the Schmalhausen Institute of Zoology of the Ukrainian Academy of Sciences in Kiev (Ukraine). Gorb's research focuses on morphology, structure, biomechanics, and evolution of surface-related functional systems in animals and plants, as well as the development of biologically inspired technological surfaces and systems. In 2018, he received Karl-Ritter-von-Frisch Medal of German Zoological Society. Gorb is a corresponding member of Academy of the Science and Literature Mainz, and member of the National Academy of Sciences Leopoldina, Germany.